CLASP2 interacts with p120-catenin and governs microtubule dynamics at adherens junctions

Marta N. Shahbazi,[1] Diego Megias,[2] Carolina Epifano,[1] Anna Akhmanova,[3] Gregg G. Gundersen,[4] Elaine Fuchs,[5] and Mirna Perez-Moreno[1]

[1]Epithelial Cell Biology Laboratory, BBVA (Banco Bilbao Vizcaya Argentaria) Foundation–CNIO (Spanish National Cancer Research Center) Cancer Cell Biology Program; and [2]Confocal Microscopy Unit, Biotechnology Program; CNIO, 28029 Madrid, Spain
[3]Cell Biology, Faculty of Science, Utrecht University, 3584 CH Utrecht, Netherlands
[4]Department of Pathology and Cell Biology, Columbia University, New York, NY 10027
[5]Laboratory of Mammalian Cell Biology and Development, Howard Hughes Medical Institute, The Rockefeller University, New York, NY 10065

Classical cadherins and their connections with microtubules (MTs) are emerging as important determinants of cell adhesion. However, the functional relevance of such interactions and the molecular players that contribute to tissue architecture are still emerging. In this paper, we report that the MT plus end–binding protein CLASP2 localizes to adherens junctions (AJs) via direct interaction with p120-catenin (p120) in primary basal mouse keratinocytes. Reductions in the levels of p120 or CLASP2 decreased the localization of the other protein to cell–cell contacts and altered AJ dynamics and stability. These features were accompanied by decreased MT density and altered MT dynamics at intercellular junction sites. Interestingly, CLASP2 was enriched at the cortex of basal progenitor keratinocytes, in close localization to p120. Our findings suggest the existence of a new mechanism of MT targeting to AJs with potential functional implications in the maintenance of proper cell–cell adhesion in epidermal stem cells.

Introduction

Throughout the eukaryotic kingdom, the microtubule (MT) cytoskeleton functions in a wide range of fundamental physiological processes, including organelle positioning, mitosis, cell polarity, and migration (Olmsted and Borisy, 1973). In all these contexts, it is crucial that this dynamic cytoskeleton is precisely organized to preserve cellular functions. MTs are polarized polymers with a minus end anchored to an MT-organizing center, being usually the centrosome (Lüders and Stearns, 2007). MTs radially grow from the MT-organizing center projecting their plus ends toward the cell membrane and recurrently undergo stochastic switches of growth and shrinkage, a process termed dynamic instability (Desai and Mitchison, 1997; Howard and Hyman, 2009). Capture of MT plus ends at cortical sites leads to a decrease in MT dynamic instability (Gundersen, 2002). Epithelial cells also develop noncentrosomal MTs that generally orient their minus ends toward the apical domain, and their plus ends extend laterally toward the basal domain (Bacallao et al., 1989; Bartolini and Gundersen, 2006).

Previous findings have illustrated a dynamic cross talk between cadherins and MTs (Chausovsky et al., 2000; Waterman-Storer et al., 2000). Cadherin-mediated adhesion through adherens junctions (AJs) stabilizes MTs (Waterman-Storer et al., 2000) and is sufficient for their recruitment (Stehbens et al., 2006). Moreover, subsets of both MT plus ends (Ligon et al., 2001; Stehbens et al., 2006) and minus ends (Meng et al., 2008; Bellett et al., 2009) have been observed at AJs. Conversely, MT depolymerization has a negative effect on cadherin stability (Yap et al., 1995) and formation (Mary et al., 2002) but also on AJ disassembly (Ivanov et al., 2006), depending on the cell context. MT plus end–tracking proteins (+TIPs; Akhmanova and Steinmetz, 2008) have been associated to AJs (Akhmanova et al., 2009). For example, dynein binds to the AJ protein β-catenin (Ligon et al., 2001), and CLIP-170 localizes near cadherin clusters (Stehbens et al., 2006). That said, the molecular players

Correspondence to Mirna Perez-Moreno: maperez@cnio.es

Abbreviations used in this paper: AJ, adherens junction; ECad, E-cadherin; Fc, fragment crystallizable; KO, knockout; LC, low calcium; mKer, mouse keratinocytes; MT, microtubule; NC, normal calcium; PCad, P-cadherin; ROI, region of interest; +TIP, plus end–tracking protein; TOG, tumor overexpressed gene; WT, wild type.

The Rockefeller University Press $30.00
J. Cell Biol. Vol. 203 No. 6 1043–1061
www.jcb.org/cgi/doi/10.1083/jcb.201306019

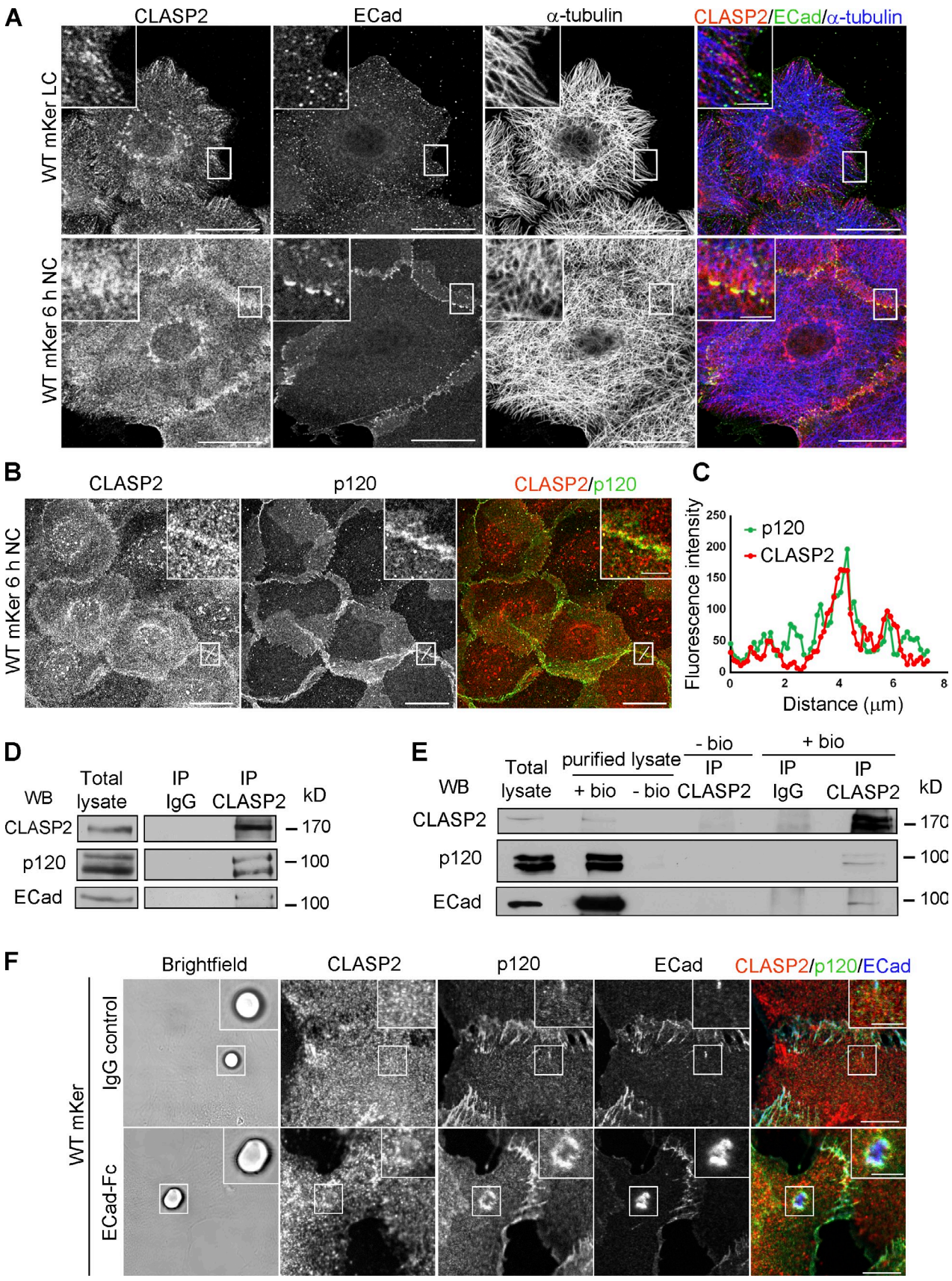

Figure 1. **CLASP2 and p120 interact at AJs.** (A) WT primary mKer were grown in low confluency to allow the formation of colonies. Cells were immunostained for CLASP2, ECad, and α-tubulin in the presence or absence of calcium (NC, normal calcium; LC, low calcium). (B) WT primary mKer immunostained for CLASP2 and p120 in the presence of calcium to induce formation of AJs. (C) Plot profile of CLASP2 and p120 fluorescence intensity

underlying the MT–AJ connection and their physiological significance in tissue homeostasis are still unfolding.

Best known for its role as a regulator of cadherin stability at the cell membrane (Davis et al., 2003; Ishiyama et al., 2010), the AJ protein p120 is a strong candidate for regulating MT–AJ dynamics. p120 has been reported to associate with MTs in a cadherin-independent manner (Franz and Ridley, 2004; Yanagisawa et al., 2004; Ichii and Takeichi, 2007). However, when bound to cadherins, p120 has been found to associate with the protein PLEKHA7, which in turn recruits the MT minus end–binding protein Nezha, leading to anchorage of MTs at mature AJs (Meng et al., 2008).

One of the current challenges in the field is to determine which molecular interactions take place between MTs and AJs in primary cells and tissues and how they preserve cellular functions within a physiological context. During terminal differentiation in the stratified epidermis, MTs in suprabasal cells reorganize in a desmosome-dependent manner into cortical noncentrosomal arrays (Lechler and Fuchs, 2007; Simpson et al., 2011; Sumigray et al., 2011, 2012). In contrast, mitotically active basal progenitors, which adhere through integrins to an underlying basement membrane of extracellular matrix proteins, display a paucity of desmosomes, and their lateral intercellular junctions are largely composed of AJs. Whether and/or how MTs are targeted to AJs in these basal stem cells is unknown. Here, we report that the +TIP protein CLASP2 (CLIP-associated protein 2) localizes to AJs via p120 in primary basal mouse keratinocytes (mKer), and this interaction changes upon commitment to terminal differentiation. Our findings provide a new mechanism of MT targeting to AJs, with potential functional implications in the maintenance of proper cell–cell adhesion in epidermal stem cells.

Results

CLASP2 and p120 interact at AJs in primary mKer

The interaction between p120 and CLASP2 was initially identified in a yeast two-hybrid assay, screening a mouse skin cDNA expression library with the p120 N-terminal domain as bait (1–467 aa), in which 6% of the clones identified corresponded to CLASP2 (unpublished data). CLASP2 was first described as a CLIP-170 and CLIP-115 binding partner (Akhmanova et al., 2001), which stabilizes MT plus ends at the cell cortex (Mimori-Kiyosue et al., 2005; Drabek et al., 2006). As such, this made it a potential candidate to couple MTs to intercellular junctions. To pursue this notion, we first validated the results obtained with the yeast-two hybrid in mKer. For this purpose, we generated a CLASP2 rabbit polyclonal antibody against the C-terminal region of the protein (Akhmanova et al., 2001). The specificity of this antibody was tested by peptide competition assays (Fig. S1, A and B) and was further validated in knockdown experiments presented later in this paper (see Fig. 5 B).

When mKer were cultured under low calcium (LC) conditions, CLASP2 decorated MT plus ends at the cortex as expected. It also localized to perinuclear regions in agreement with previous results documenting its localization at the Golgi (Efimov et al., 2007; Miller et al., 2009). Under these conditions, E-cadherin (ECad) was not found at junctional sites (Fig. 1 A). After promoting AJ formation in mKer upon calcium switch (Vasioukhin et al., 2000), CLASP2 redistributed to areas of ECad puncta, whereas at cell-free edges, CLASP2 maintained the typical MT plus end–tracking pattern (Fig. 1 A). Supporting these observations, ECad/P-cadherin (PCad) double-deficient mKer (Tinkle et al., 2008) failed to concentrate CLASP2 at the cortex but not CLASP2 localization on MT plus ends (Fig. S1 C).

At cell–cell adhesion sites in wild-type (WT) mKer, CLASP2 and p120 colocalized as judged by immunofluorescence analyses (Fig. 1, B and C). Suggestive of specificity, such robust interaction was not observed at other cell sites under LC conditions by immunofluorescence or immunoprecipitation (Fig. S1, D–F). To test whether CLASP2 and p120 physically interact, CLASP2 was immunoprecipitated from mKer after 6 h of calcium treatment. The immunoprecipitates contained p120 as well as ECad (Fig. 1 D). To demonstrate that this complex exists at the membrane, we isolated biotinylated surface proteins using a streptavidin pull-down purification strategy. CLASP2 was detected in the purified lysate of surface proteins and coimmunoprecipitated with p120 and ECad (Fig. 1 E). In addition, we used time-lapse video microscopy to study the dynamic behavior of CLASP2 at sites of cell–cell adhesion in WT mKer. We observed GFP-CLASP2 comets moving continuously toward regions of cell–cell adhesion as marked by p120-cherry. Upon reaching these areas, many of these CLASP2 comets traveled along the AJs, suggesting an interaction of CLASP2 with junctional components (Video 1). Collectively, these results indicate that CLASP2–p120–ECad form an intercellular complex within cells of an epidermal sheet.

To determine whether ECad-mediated intercellular adhesion was sufficient to promote the recruitment of CLASP2 to adhesion sites, we incubated mKer with microspheres coated with recombinant fragment crystallizable (Fc)–ECad (Chappuis-Flament et al., 2001) and observed an enrichment of both CLASP2 and p120 around the adhesion sites (Fig. 1 F). All together, these observations point to a model in which CLASP2 and p120 interact at sites of cell–cell adhesion in primary mKer in an ECad-dependent manner.

at AJs in the area indicated in B. (D) CLASP2 was immunoprecipitated from mKer treated with calcium, and the immunoprecipitates (IP) were analyzed for CLASP2, ECad, and p120 by immunoblotting. Rabbit IgGs were used as a control. (E) Cell surface proteins from mKer treated with calcium were labeled with biotin (bio) and purified with a streptavidin column. CLASP2 was immunoprecipitated from the purified lysate of surface proteins, and CLASP2, p120, and ECad were analyzed by immunoblotting. Rabbit IgGs were used as a control of the immunoprecipitation, and a lysate of cells without biotin was used as a control of the purification. (F) WT mKer incubated with ECad-Fc–coated microspheres for 5 h in the presence of calcium. IgG-coated microspheres were used as a control. Cells were immunostained for CLASP2, p120, and ECad. Insets are magnifications of the boxed regions. WB, Western blot. Bars: (A and B, main images) 25 µm; (F) 10 µm; (A, B, and F, insets) 5 µm.

The N-terminal domain of p120 and the Ser/Arg-rich domain of CLASP2 mediate their direct interaction

To analyze the mechanism by which p120 recruits CLASP2 to cortical sites, we first explored whether this interaction occurs in a direct manner followed by the identification of the specific domains responsible of their interaction. To this end, we generated a series of GST-tagged CLASP2 and p120 recombinant proteins (Fig. 2 A) and confirmed their expression by SDS-PAGE and immunoblotting (Figs. 2 B and S2). Using pull-down assays, we showed that all three recombinant GST-CLASP2 proteins directly interacted with p120 full length (p120FL). In contrast, a mutant p120 protein lacking the N-terminal domain (p120ΔN) showed no association with CLASP2 (Fig. 2 C). Furthermore, the N-terminal domain of p120 alone (p120N) was sufficient to interact directly with the three GST-CLASP2 constructs generated (Fig. 2 D). These results validate the yeast two-hybrid data and show that the N-terminal regulatory domain of p120 is responsible for the interaction between CLASP2 and p120 (Fig. S2 D). We also observed that the three recombinant GST-CLASP2 proteins interacted with endogenous p120 present in protein lysates from primary mKer that were isolated 4 h after calcium switch (Fig. 2 E).

We further pursued the identification of the specific CLASP2 domain responsible of the interaction with p120N by using a series of GFP-tagged CLASP2 deletion mutant proteins (Fig. 2 F; Mimori-Kiyosue et al., 2005). The constructs were expressed in 293T cells, and protein lysates containing equal amounts of each fusion protein were incubated with the recombinant GST-p120N fragment purified in vitro. These experiments revealed that from the different constructs tested, a robust interaction was only observed between p120N and the CLASP2 mutant CLASP2N1 (Fig. 2 G), which contains a Ser/Arg-rich region and a tumor overexpressed gene (TOG)–like domain (Fig. 2 F). To further dissect the region responsible for the interaction within the CLASP2N1 sequence, a construct that lacks the Ser/Arg–rich region and a construct that contains the TOG-like domain were used. Interestingly, the lack of the Ser/Arg-rich region impaired the robust interaction observed with the CLASP2N1 recombinant protein (Fig. 2 G). In addition, the TOG-like domain did not interact, indicating that the binding site for p120 is located within the Ser/Arg-rich region (Fig. 2 H). Because it has been previously documented that the C-terminal domain of CLASP2 can bind indirectly to MTs via CLIP-170 (Akhmanova et al., 2001; Mimori-Kiyosue et al., 2005), our results raise the possibility that through its Ser/Arg-rich region, CLASP2 can bind to p120, serving as a bridge to target MTs to AJs.

p120 is required for proper localization of CLASP2 at AJs

To test whether CLASP2 localization to AJs depends on p120, we isolated primary mKer from the back skin of newborn p120 conditional knockout (KO) mice in which p120 ablation was specifically and efficiently targeted in skin epidermis (Perez-Moreno et al., 2006). We confirmed that p120 deficiency leads to a delay in AJ formation in mKer in vitro as previously described (Perez-Moreno et al., 2006). CLASP2 total levels were not affected (Fig. S3 A), but its distribution was specifically lost at cell–cell contacts in p120 KO mKer when compared with controls after 6 h of calcium switch (Fig. 3, A and B). Incubation with calcium for 12 h was associated with the establishment of areas of cadherin-mediated adhesion and a weak recruitment of CLASP2 to these sites (Fig. S3 B). Importantly, p120 deficiency did not impair CLASP2 localization to MT plus ends at cell-free edges (Fig. S3 C) or at the Golgi (Fig. S3 D).

To study the cell-autonomous events upon p120 ablation, we isolated p120 flox/flox ($p120^{f/f}$) mKer from the back skin of newborn mice and performed gene recombination in vitro using adenoviruses (adeno) expressing Cre-GFP recombinase ($p120^{\Delta/\Delta}$ mKer). Primary mKer transduced with adeno-GFP were used as controls ($p120^{f/f}$). We first confirmed the ablation of p120 by immunoblotting (Fig. 3 C) and also observed that loss of p120 did not lead to changes in the total levels of CLASP2 (Fig. 3 D). Next, we immunoprecipitated ECad from both control and p120-null mKer and validated that CLASP2 failed to co-immunoprecipitate with ECad in the absence of p120 (Fig. 3 D).

These results suggest that p120 is required for CLASP2 localization to AJs. However, p120-null mKer also had reduced levels of ECad (Fig. 3 A), raising the possibility that this defect was responsible for the reduced CLASP2 enrichment at AJs. To test this possibility, we performed rescue assays with p120. Expression of p120 full length–HA (p120FL-HA) rescued the localization of CLASP2 and ECad to AJs as assayed by immunofluorescence (Fig. 3, E and F). However, expression of p120ΔN-HA, which does not bind CLASP2, rescued the levels of ECad but not those of CLASP2 at AJs (Fig. 3, E and F). In addition, we overexpressed ECad-HA to promote its accumulation at the membrane in both control and p120-null mKer. Despite the increased presence of ECad at the membrane, CLASP2 levels at AJs after 6 h of calcium switch remained lower in p120-null cells when compared with controls (Fig. S3, E and F).

Overall, these data provide compelling evidence that p120 is required to localize CLASP2 to AJs in a normal physiological context. These results validate our pull-down experiments and demonstrate that the N-terminal domain of p120 is required to localize CLASP2 at AJs. That said, ectopic overexpression of ECad-HA led to a partial recruitment of CLASP2 when compared with p120-null cells (Fig. 3 B), suggesting that there may be additional mechanisms that can recruit CLASP2 to cell–cell contacts when p120 is absent and ECad levels are atypically high.

CLASP2 is present at AJs either associated to MTs or independently of MTs

To analyze the connections of CLASP2 with both MTs and ECad adhesion sites, we analyzed CLASP2 distribution after 1 h of calcium treatment. Under these settings, CLASP2 was found at MT plus ends that were reaching ECad puncta (Fig. 4 A). To assess whether stable MTs were also decorated by CLASP2 at AJs, we treated cells with a low dose (5 µM) of nocodazole. After 30 min of nocodazole treatment, CLASP2 was still present at the tips of MTs that were stabilized at ECad adhesion sites (Fig. 4 B).

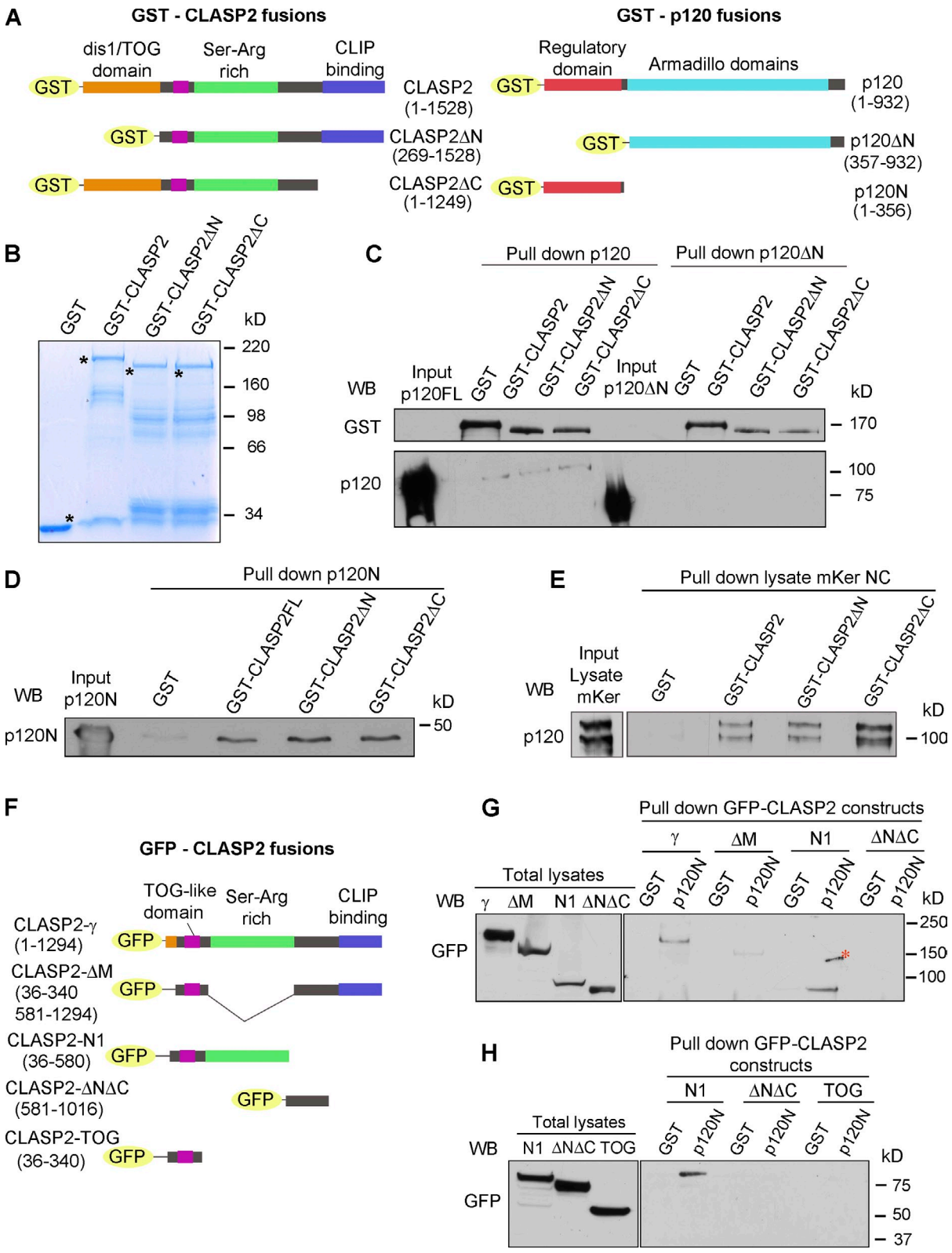

Figure 2. **p120 and CLASP2 interact via the N-terminal domain of p120 and the Ser/Arg-rich region of CLASP2.** (A) GST-tagged constructs of p120 and CLASP2 used for the in vitro pull-down assays. (B) SDS-PAGE gel showing the purified GST-CLASP2 recombinant proteins stained with Coomassie blue. Asterisks indicate bands of the expected molecular mass. (C) In vitro binding assay of GST-CLASP2 recombinant proteins with purified p120FL and p120ΔN (previously cleaved from GST with the PreScission Protease). (D) In vitro binding of GST-CLASP2 recombinant proteins with purified p120N. (E) Pull-down assay using the recombinant GST-CLASP2 proteins as bait for endogenous p120 present in lysates of mKer treated with calcium for 4 h. (E) GFP-tagged constructs of CLASP2. (F) Pull-down assays using GST-p120N recombinant protein and lysates of 293T cells expressing equal amounts of the GFP-tagged CLASP2 constructs of E. Pulled down proteins were immunoblotted for GFP. (H) Pull-down assay using GST-p120N recombinant protein and lysates of 293T cells expressing equal amounts of either GFP–CLASP2-N1 or GFP–CLASP2-ΔNΔC or GFP–CLASP2-TOG. WB, Western blot.

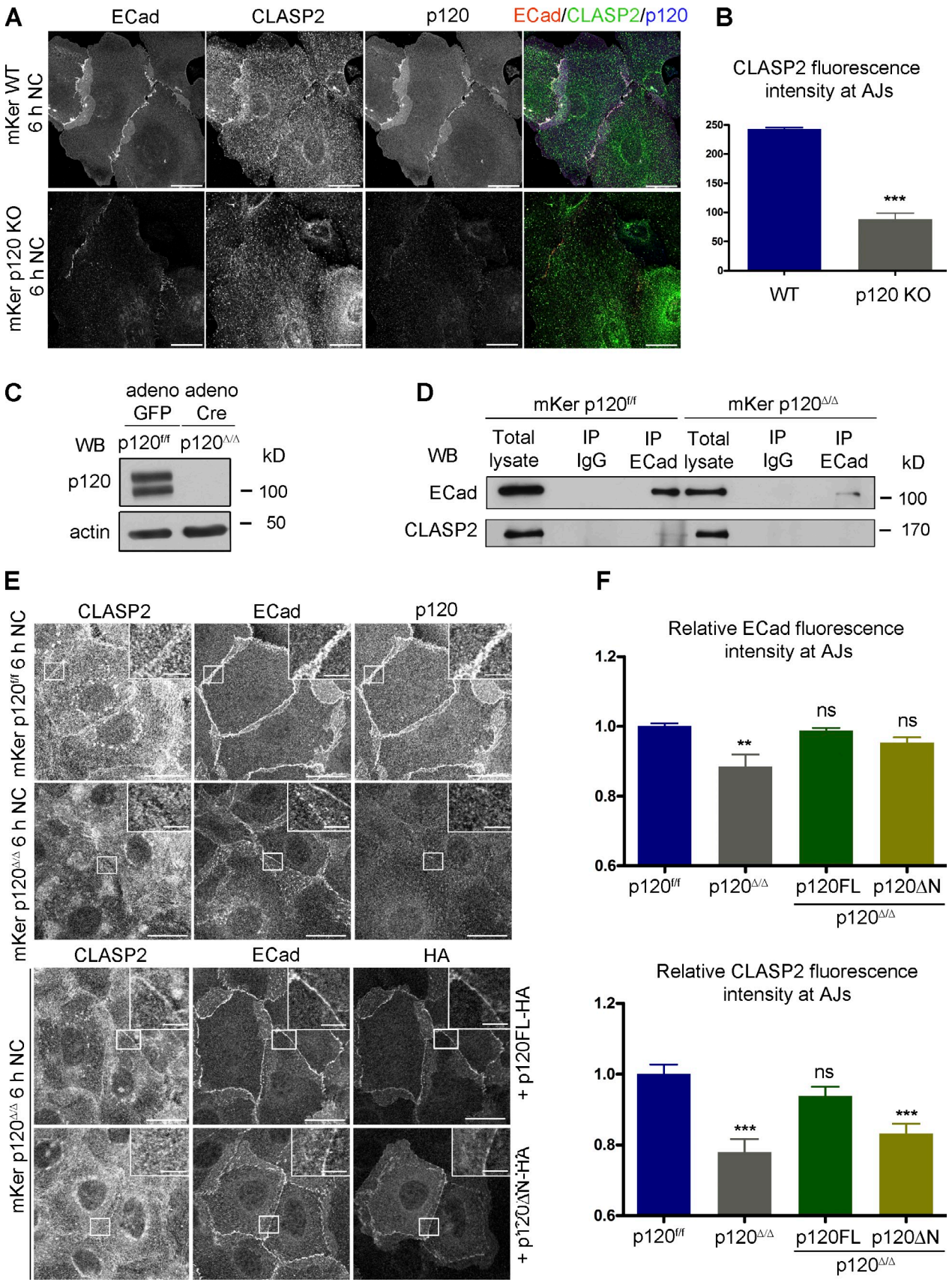

Figure 3. **p120 is required for the recruitment of CLASP2 to AJs.** (A) WT and p120 KO primary mKer immunostained for ECad, CLASP2, and p120 in the presence of calcium (NC). (B) Random individual plot profiles (n = 10 per cell/10 cells) were obtained from WT and p120 KO mKer. The fluorescence intensity level of CLASP2 corresponding to the maximum ECad intensity in each profile was quantified. Data are represented as means ± SEM;

Next, we evaluated whether the capture of CLASP2 at AJs was stable even after disruption of MTs. To this end, we induced AJ formation with calcium and then treated WT primary mKer with high doses (30 µM) of nocodazole. Under these conditions, nocodazole fully depolymerized the MT network within 4 h of treatment, as observed after extraction of monomeric tubulin (Fig. S4 A; Gundersen et al., 1987). In the absence of calcium, nocodazole treatment did not lead to AJ formation in our system, counter to previous observations made with human keratinocytes (Fig. S4 B; Kee and Steinert, 2001).

As judged by immunofluorescence, CLASP2 remained at AJs despite the absence of MTs (Fig. 4 C). Quantification of CLASP2 levels showed a 30% decrease in the levels of CLASP2 at cell–cell adhesion sites after 2–4 h of treatment with nocodazole (Fig. 4 D). Concomitantly, ECad levels at the membrane were stabilized, suggesting that AJs cannot be disassembled in the absence of MTs as previously described (Ivanov et al., 2006). Coimmunoprecipitation experiments revealed that CLASP2, p120, and ECad still formed a complex in the absence of MTs (Fig. 4 E).

Overall, these results suggest that CLASP2 may function as a bridge linking MTs to AJs via p120. The fact that CLASP2 remains at AJs after depolymerization of MTs suggests that CLASP2 is highly stabilized at AJs, through its association with p120 and possibly other cytoskeletal interactions (e.g., actin; Tsvetkov et al., 2007).

Loss of CLASP2 leads to a delay in AJs formation and impairs AJ stability and function

To analyze the functional relevance of CLASP2 in the regulation of AJs, we performed in vitro loss of function experiments. The expression of CLASP2 in mKer was knocked down by transducing cells with lentiviruses containing a specific shRNA. The knockdown efficiency was very high (98%), as observed by immunofluorescence and Western blotting (Fig. 5, A and B). The total levels of AJ proteins did not change in the absence of CLASP2 (Fig. 5 C). Monolayers looked less compact, and cell size was bigger (Fig. 5 D). The recruitment of p120 (Fig. 5, D and E), α-catenin, and ECad (Fig. 5, F and G) to adhesion sites was delayed starting from early stages of junction formation upon stimulation with calcium, when compared with the scramble controls (Fig. 5 D). This was not caused by an impairment of p120 to associate with ECad (Fig. S5 C). Overall, these data suggest that CLASP2 may function in the proper formation and maintenance of AJs. Because mammalian CLASP2 and CLASP1 proteins play redundant roles in different cellular functions (Mimori-Kiyosue et al., 2005), we further tested whether CLASP2 deficiency led to an increase in CLASP1 levels in mKer. No changes in CLASP1 levels were observed under these conditions (Fig. S5 B). In addition, unlike CLASP2, CLASP1 was only moderately localized at the cortex near adhesion sites (Fig. S5 C). However, CLASP1 deficiency led to a delay in the formation of AJs upon calcium switch without altering the expression levels of AJ proteins (Fig. S5, C and D), suggesting that both proteins may cooperate in the formation of AJs. Indeed, their double deletion produced a much stronger AJ phenotype (Fig. S5 E).

To probe more deeply into how loss of CLASP2 affects p120 dynamics at the membrane, we used FRAP microscopy. In brief, control and CLASP2-deficient mKer were transfected with a p120-cherry expression vector. FRAP was performed on cells displaying comparable levels of p120-cherry at sites of cell–cell contacts. As shown in Fig. 6 A, recovery of p120 fluorescence intensity was markedly reduced in CLASP2-deficient mKer when compared with control cells. Appreciable decreases were measured both in the half-life and in the mobile fraction of the protein, suggesting a problem with the delivery or recycling of AJ components (Table S1).

To evaluate the ability of CLASP2-deficient mKer to establish functional ECad-mediated adhesions, cells were seeded onto plates coated with Fc-ECad (Chappuis-Flament et al., 2001) and incubated under normal calcium (NC) conditions for either 30 or 60 min, and nonattached mKer were washed out. In comparison to controls, fewer CLASP2-deficient mKer remained attached to the plates (Fig. 6 B).

To probe further into the functional relevance of the CLASP2 interaction with AJs, we analyzed AJ stability by removing calcium from epithelial sheets of CLASP2-deficient and control mKer. Calcium removal is known to induce ECad internalization and AJ disassembly. 30 min after removal of calcium, AJs in WT cells were visibly affected, and CLASP2 was found in close proximity to the cortex concentrated at MT plus ends in certain areas (Fig. 6 C). In the case of CLASP2-deficient mKer, 30 min of calcium withdrawal were sufficient to induce cell–cell detachment, although some positive areas for ECad were still observed at the membrane (Fig. 6 C). Overall, these data show that CLASP2 is required to maintain the adequate adhesive properties of AJs in proliferative progenitor mKer.

CLASP2 deficiency leads to a decrease in MT density and stability at AJ

It has previously been reported that MTs regulate ECad dynamics at cell–cell contacts. In particular, treatment with nanomolar concentrations of nocodazole, which disrupts MT plus-end dynamics, leads to a decrease in the concentration of ECad at the

***, P < 0.0001, Mann–Whitney *U* test. (C) Western blot (WB) showing the levels of p120 in primary mKer infected either with adeno-GFP ($p120^{f/f}$) as a control or adeno-Cre-GFP ($p120^{\Delta/\Delta}$). (D) ECad was immunoprecipitated from control $p120^{f/f}$ or from p120-null mKer ($p120^{\Delta/\Delta}$). The immunoprecipitates (IP) were analyzed for ECad and CLASP2 by immunoblotting. (E) $p120^{\Delta/\Delta}$ mKer were transfected with either p120FL-HA or p120ΔN-HA and switched to a normal calcium media (NC) for 6 h. $p120^{f/f}$ and $p120^{\Delta/\Delta}$ mKer nontransfected were used as controls. Cells were immunostained for CLASP2, ECad, and HA. Insets are magnifications of the boxed regions. (F) Quantification of ECad and CLASP2 fluorescence intensity at AJs. Random individual plot profiles were generated at sites of cell–cell adhesion. The maximum value of ECad fluorescence intensity in the profile and its associated CLASP2 fluorescence intensity were quantified. Data were normalized to control values ($p120^{f/f}$ mKer) and represented as means ± SEM. **, P < 0.002, Mann–Whitney *U* test for ECad; ***, P < 0.0003, Student's *t* test for CLASP2 (10 plot profiles per cell and 16 cells per condition). Bars: (A and E, main images) 25 µm; (E, insets) 5 µm.

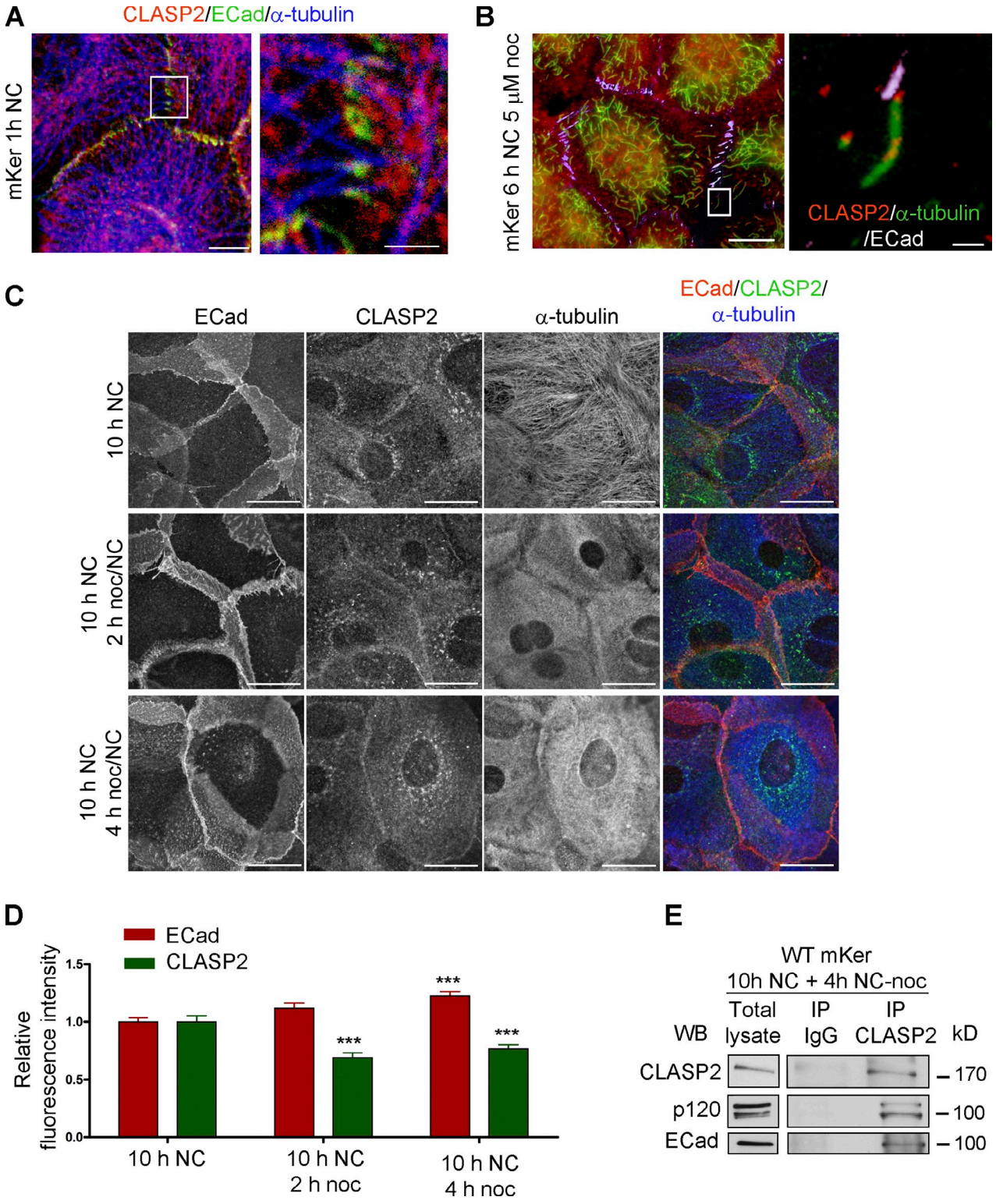

Figure 4. **CLASP2 is present at AJs either associated to MTs or in an MT-independent manner.** (A) WT mKer were treated with calcium for 1 h and immunostained for CLASP2, ECad, and α-tubulin. The right image is a higher magnification of the selected region. (B) WT mKer were treated with calcium for 4 h followed by treatment with 5 μM nocodazole (noc) for 30 min and extraction of monomeric tubulin with saponin. Cells were immunostained for ECad, CLASP2, and α-tubulin. The right image is a higher magnification of the selected region. (C) WT primary mKer were treated with calcium (NC) for 10 h as a control followed by treatment with nocodazole + calcium for 2, 4, or 8 h. Cells were immunostained for ECad, CLASP2, and α-tubulin. (D) Random individual plot profiles at cell–cell adhesion sites (n = 10 per cell/40–50 cells) were obtained for the different time points of nocodazole treatment. The maximum fluorescence intensity of ECad and CLASP2 for each profile was quantified and normalized to the control not treated with nocodazole. Data are represented as means ± SEM. ***, $P < 0.0001$, Mann–Whitney U for ECad; ***, $P < 0.001$, Student's t test for CLASP2. (E) CLASP2 was immunoprecipitated from mKer treated with calcium for 10 h followed by treatment with nocodazole + calcium for 4 h. The immunoprecipitates (IP) were analyzed for CLASP2, p120, and ECad by immunoblotting. WB, Western blot. Bars: (A, main image) 7.5 μm; (A, inset) 2 μm; (B, main image, and C) 25 μm; (B, inset) 5 μm.

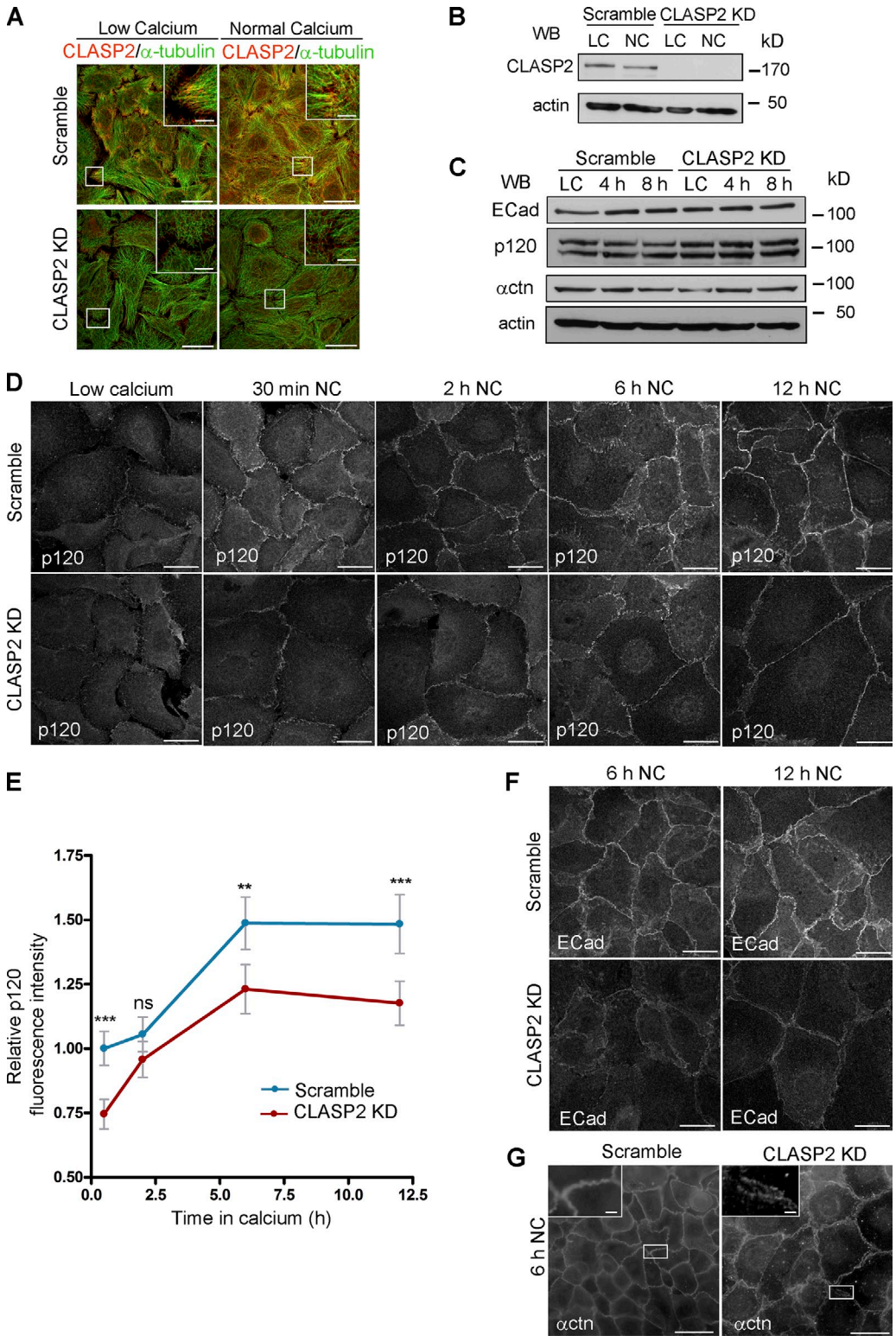

Figure 5. **CLASP2 is required for the proper formation of AJs.** (A) WT mKer were infected with lentiviruses expressing either CLASP2 shRNA (CLASP2 knockdown [KD]) or scramble shRNA (scramble). The levels of CLASP2 were analyzed by immunofluorescence after selection with G418. (B) Western blot (WB) showing the levels of CLASP2 after infection with the corresponding lentiviruses. (C) Western blot showing the total levels of ECad, p120, and α-catenin (αctn) in scramble and CLASP2 knockdown mKer at different time points of a calcium-switch time course experiment. (D) Scramble and CLASP2-deficient mKer were subjected to calcium switch for 30 min, 2 h, 6 h, and 12 h and immunostained for p120. (E) Quantification of p120 levels at the membrane in scramble and CLASP2-deficient mKer. Random individual plot profiles were generated at sites of cell–cell adhesion (10 per cell, 25–35 cells), and the maximum fluorescence intensity was quantified. Data are normalized to scramble control values after 30 min of calcium treatment and represented as means ± SEM; **, $P < 0.003$; ***, $P < 0.0001$, Mann–Whitney *U* test. (F) Scramble and CLASP2-deficient mKer treated with calcium for either 6 or 12 h and immunostained for ECad. (G) Scramble and CLASP2-deficient mKer immunostained for α-catenin after 6-h calcium switch. Insets are magnifications of the boxed regions. Bars: (A, main images, D, and F) 25 µm; (G, main images) 50 µm; (A and G, insets) 5 µm.

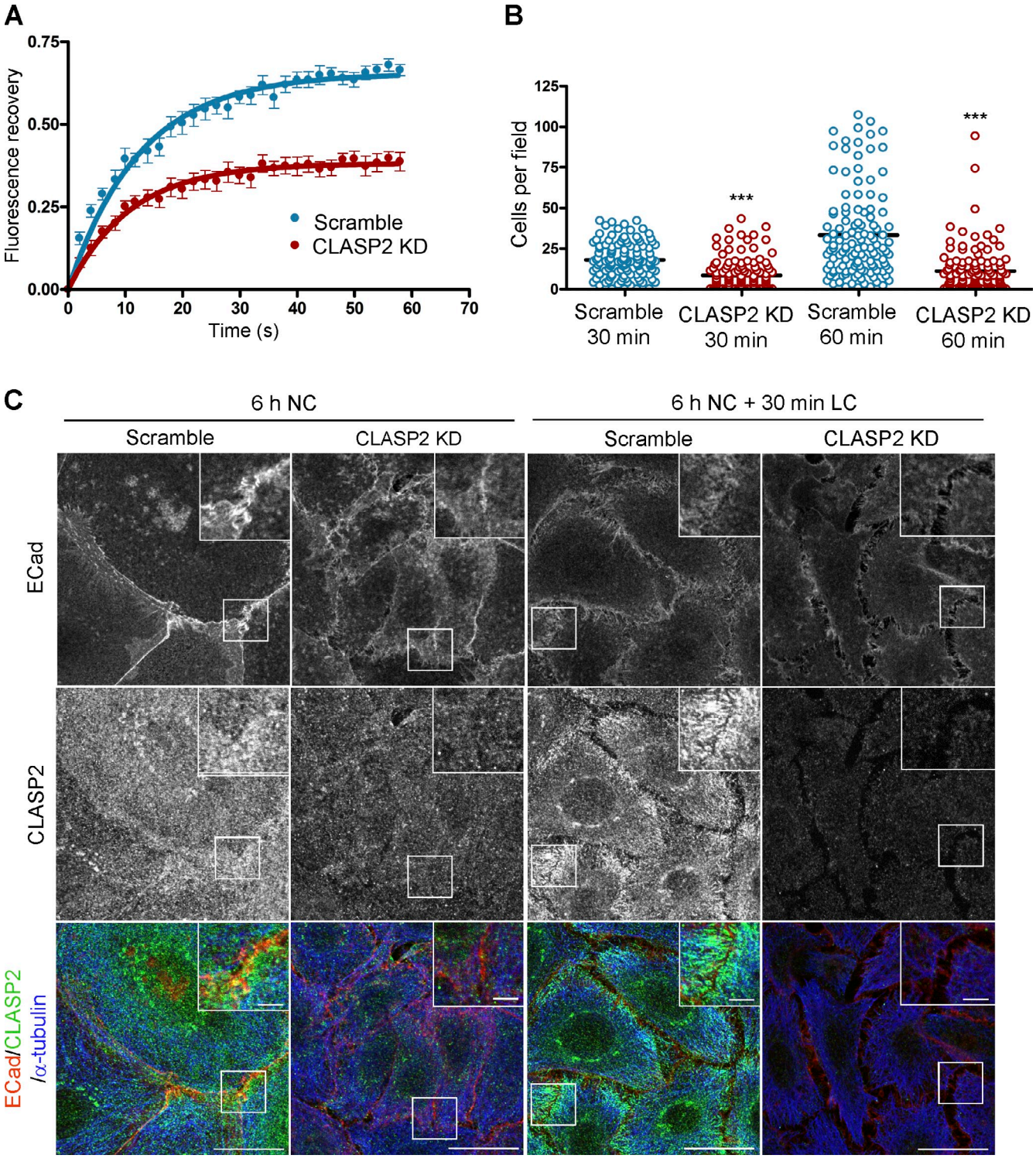

Figure 6. **CLASP2 is required to maintain the proper dynamics and functionality of AJs.** (A) Graph showing the fluorescence recovery after photobleaching of p120-cherry in a ROI selected at an area of cell–cell contact, in both scramble and CLASP2 knockdown (KD) mKer. Dots represent arithmetic means ± SEM, and solid lines are best-fit single exponential curves. Data were normalized to prebleach and postbleach values. (B) CLASP2-deficient mKer and their WT counterparts (scramble) were allowed to attach to Fc-ECad–coated plates for 30 min and 1 h. After the removal of nonadhered cells, the number of cells attached to the plates was quantified in several fields (n = 3 independent experiments, 40 images per experiment). As negative controls, plates coated with mouse Fc and mKer in the presence of EDTA were used. Data are represented as means ± SEM; ***, $P < 0.0001$, Mann–Whitney U test. (C) CLASP2-deficient mKer and their WT counterparts (scramble) were treated for 6 h with calcium to induce AJ formation. Calcium was removed from the cell culture media to induce AJ disassembly, and 30 min after, cells were fixed and immunostained for ECad, CLASP2, and α-tubulin. Insets are magnifications of the boxed regions. Bars: (main images) 25 µm; (insets) 5 µm.

membrane in MCF-7 cells (Stehbens et al., 2006). These results are similar to our observations indicating that loss of CLASP2 decreases the recruitment of p120 to the membrane. Thus, we reasoned that altered MT dynamics and/or decreased MT targeting to cell–cell contacts as a consequence of CLASP2 deficiency could be responsible for the decreased dynamics of p120 at the membrane. To test this hypothesis, we began by analyzing the MT network in fixed cells that had been treated with calcium to induce AJ formation. We quantified the number of MT targeting events at cell–cell contacts by counting the number of MTs that reached areas of ECad-mediated cell–cell adhesion. This analysis revealed first that both CLASP2-deficient and p120-null cells had fewer MTs per AJ area than controls (Fig. 7, A and B) and second that they were more susceptible to nocodazole depolymerization (Fig. 7, C and D).

To gain a deeper understanding of MT behavior in the absence of CLASP2 and p120, we tried to analyze MT dynamics at AJs in cells stably expressing cherry-tubulin. However, because of the high density of MTs at AJs, we were unable to follow individual MT ends. For this reason, we analyzed plus-end MT dynamics expressing the recombinant +TIP protein EB3-GFP (Stepanova et al., 2003). EB3 comets moved toward cell–cell contacts and disappeared upon reaching AJs, possibly as a result of pausing and stabilization of the MT, although MT catastrophe cannot be ruled out. Control cells showed a progressive decrease in the speed of EB3-GFP comets as they reached the junction (Fig. 7 E). The speed of EB3-GFP comets in CLASP2-deficient cells was increased at all time points, which may indicate that MTs do not properly pause at AJs in the absence of CLASP2 (Fig. 7 E). Interestingly, EB3-GFP comets in p120-null mKer showed the same increase in overall growth rate as observed in the absence of CLASP2 (Fig. 7 E and Table 1). Reflecting the fact that MT growth is faster in the vicinity of AJs both in p120-null and CLASP2-deficient cells, the total distance covered by individual growing MTs during the 12 s analyzed was also significantly higher when compared with controls (Table 1). These results are consistent with the concept that decreases in MT density are connected with increases in MT growth caused by an increment of tubulin dimers (Mimori-Kiyosue et al., 2005).

We further analyzed the tracks of individual MTs during the last 12 s before they reach the AJs. To this end, the positions in the xy plane at the different time points were normalized to the final position corresponding to the moment in which the EB3-GFP comets reach the AJs. After this approach, we observed that both in CLASP2-deficient and p120-null mKer, EB3-GFP comets presented random trajectories and, in many cases, did not follow a straight path toward the junction (Fig. 7, F and G).

The fact that CLASP2 overexpression stabilizes MTs technically precluded the possibility to perform rescue experiments to test whether the alterations observed in the MTs were caused by a lack of p120–CLASP2 interaction or, alternatively, a consequence of CLASP2 deficiency by itself. However, our data do show that both CLASP2- and p120-deficient cells display an increase in the growth rate of MT plus ends at sites of cell–cell adhesion. These plus ends present random trajectories when reaching the contacts and target cell–cell contacts less frequently than controls.

CLASP2 localizes to AJs in basal progenitors of the epidermis

In vivo, p120 is present throughout the epidermis. In contrast, CLASP2 specifically localized at cortical sites in epidermal basal mKer as analyzed in newborn back skin sections (Fig. 8, A and B). These results were validated by analyzing CLASP2 expression by quantitative RT-PCR from FACS-isolated basal progenitor cells (α6 integrin^{high}) versus suprabasal terminally differentiating mKer (α6 integrin^{low}; Fig. 8 C). It was interesting to observe that the MT minus end–binding protein Nezha localized at cortical sites in the suprabasal epidermal layers (Fig. 8, A and B), consistent with the documented terminal differentiation–induced redistribution of MT minus ends (Lechler and Fuchs, 2007; Sumigray et al., 2012). Of note, we did not observe overt alterations in the distribution of CLASP2 or Nezha in p120-conditional KO epidermis (unpublished data), probably because of a compensatory action provided by ARVCF (Perez-Moreno et al., 2006), one of p120 most closely related family members (Mariner et al., 2000; Paulson et al., 2000). We also analyzed the distribution and expression of CLASP2 in vitro upon mKer differentiation. In agreement with the in vivo observations, confocal microscopy analysis of the expression of CLASP2 confirmed that it was enriched in the innermost basal cells of calcium-induced stratified primary mKer in culture (Fig. 8, D–F). The differential distribution of Nezha in suprabasal layers was also corroborated in cultured mKer that were subjected to a long treatment of calcium switch to allow the formation of suprabasal-differentiated cells (Fig. 8 D). Collectively, these results show that CLASP2 interactions with AJs are largely, if not solely, confined to basal progenitor cells of the epidermis.

Discussion

In this paper, we describe a novel and physiologically important interaction between the MT plus end–binding protein CLASP2 and the AJ component p120. This interaction leads to MT targeting to cadherin-mediated adhesions in primary mKer. In the absence of p120, CLASP2 localization to sites of cell–cell adhesion is perturbed, whereas conversely, CLASP2 deficiency alters p120 dynamics and AJ formation, stability, and function. These findings underscore a critical and hitherto unrecognized role for this MT plus end–binding protein in cell–cell adhesion.

We also discovered that absence of either CLASP2 or p120 alters MT dynamics at AJ sites. Our findings are most consistent with the notion that their coordinated interaction functions in efficient targeting of MTs to sites of cell–cell adhesion. That said, the role of p120 in the recruitment of MTs to AJs seems to be dependent on the cell context because transformed CHO cells stably expressing a mutant ECad compromised in p120 binding presented no overt alterations in MT targeting to AJs (Stehbens et al., 2006).

Overall, we propose a model in which MT targeting to AJs via the CLASP2–p120 interaction would lead to a selective MT stabilization at sites of cell–cell adhesion (Fig. 9). Based on the current data at hand, different possibilities may exist underlying the subcellular compartment in which the two proteins interact. Although p120 can bind cadherins once it

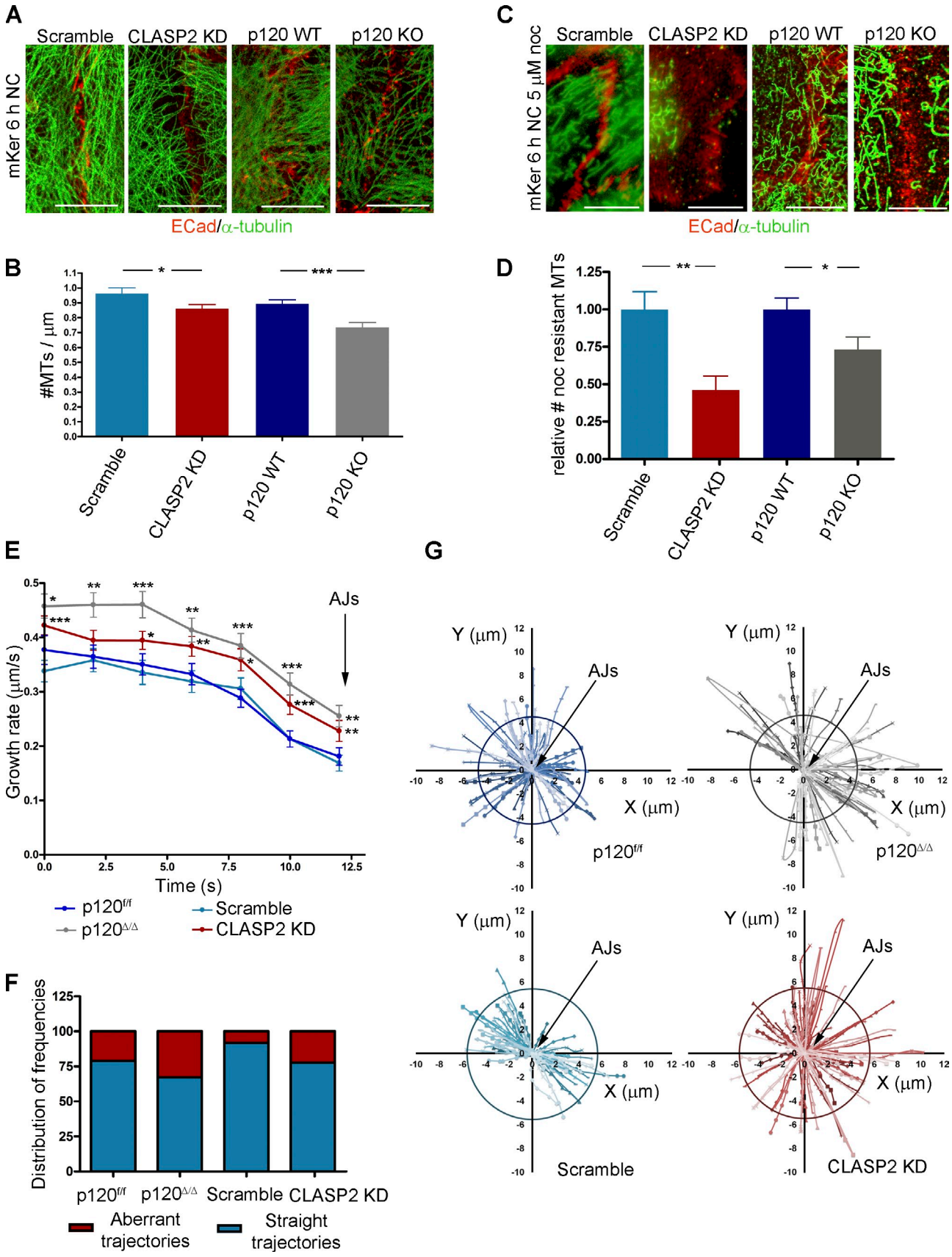

Figure 7. **CLASP2 and p120 are required to maintain the proper dynamics of MTs at cell–cell contacts.** (A) CLASP2-deficient and p120-null mKer with their corresponding scramble and p120$^{f/f}$ controls stained for ECad and α-tubulin. (B) Quantification of the number of MTs that reach an area of cell–cell contact. Only regions with well-formed AJs were selected for the analysis. (n = 60 cells, 2 independent experiments). Data are represented as means ± SEM;

Table 1. **Analysis of EB3-GFP dynamics in CLASP2-deficient and p120-null mKer with their corresponding controls**

Cell type	Number of MTs	Mean growth rate	Mean distance per MT during 12 s	Mean time in pause
		μm/s	*μm*	*s*
$p120^{f/f}$	58	0.30	5.68	2.97
$p120^{\Delta/\Delta}$	58	0.39***	8.85***	1.32*
Scramble	59	0.29	4.69	2.03
CLASP2 KD	74	0.36**	6.72***	1.17*

Summary of the data presented in Fig. 6 showing the mean growth rate, the mean distance, and the mean time in pause displayed by EB3-GFP comets in scramble control, CLASP2-deficient (CLASP2 knockdown [KD]), p120 control ($p120^{f/f}$), and p120-null ($p120^{\Delta/\Delta}$) mKer. All the analysis corresponds to the last 12 s before the MT reaches an area of cell–cell contact. Data are represented as means ± SEM. Growth rate: ***, $P < 0.001$; **, $P < 0.01$, Student's *t* test. Distance and time in pause: *, $P < 0.04$; ***, $P < 0.001$, Mann–Whitney *U* test.

reaches adhesion sites (Xiao et al., 2007), it has also been reported that p120 can bind to ECad at the Golgi (Curtis et al., 2008). Given that p120 can interact with kinesin (Chen et al., 2003; Yanagisawa et al., 2004) and that CLASP2 has a well-established role at the Golgi (Efimov et al., 2007; Miller et al., 2009), it is tempting to speculate that a CLASP2–p120–ECad complex forms at the Golgi and is subsequently delivered to the surface. If so, this would explain the delay in AJ formation that occurs in the absence of CLASP2. It would also account for the defect in AJ formation seen in p120-null mKer (Perez-Moreno et al., 2006). That said, an alternative and equally attractive model is that CLASP2 interacts with p120 upon reaching AJs, which in turn would lead to MT targeting to cell–cell contacts, thereby controlling junctional turnover at the membrane.

CLASP2 has also been implicated in targeting MTs to sites near cell matrix adhesions via the PIP3-binding proteins LL5-α and LL5-β (Lansbergen et al., 2006), promoting clustering of integrins (Hotta et al., 2010). Indeed, we see CLASP2 localized to the interface between the basal epidermal cells and its underlying basement membrane. However, the marked localization of CLASP2 to basal epidermal sites of intercellular junctions as well along with our comprehensive analyses of CLASP2's association with p120 provides a new function for CLASP2, specifically in MT targeting to AJs.

Interestingly, analogous to what has been observed in integrin-based adhesion, once CLASP2 interacts with AJs, it is stabilized even after disruption of MTs. Thus, we hypothesize that two different pools of CLASP2 may exist at AJs: an MT-independent and an MT-dependent pool. The MT-independent pool of CLASP2 could be forming additional complexes that support AJ maintenance. Consistent with this notion, we found that prolonged treatment of p120-deficient cells with calcium induced more robust AJs and was associated with a weak recruitment of CLASP2 to AJs. These experiments raise the possibility that in addition to p120, CLASP2 could interact with additional CLASP2-associated proteins that localize to AJs once they are established, such as cortical actin (Tsvetkov et al., 2007), IQGAP (Watanabe et al., 2009), 4.1R (Ruiz-Saenz et al., 2013), and ACF7 (Drabek et al., 2006; Long et al., 2013), which is known to cross-link MTs and actin at AJs in mKer (Karakesisoglou et al., 2000).

Another fascinating aspect about CLASP2 is its enrichment in the basal progenitor cells of the epidermis. Because p120 is distributed throughout the differentiated layers of the epidermis, this raises the interesting possibility that MT plus ends preferentially associate to AJs in basal progenitor cells via the CLASP2–p120 interaction (Fig. 9). In simple epithelial cells, p120 interacts with MT minus ends via a complex formed by PLEKHA7 and Nezha, leading to anchorage of MTs at mature AJs (Meng et al., 2008). This interaction occurs specifically at the zonula adherens, and not at lateral AJs, suggesting the existence of a compartmentalization of MTs at different adhesion sites. Interestingly, both CLASP2 and Nezha interact with p120 through the N-terminal domain, but we found Nezha localized in the suprabasal differentiated layers of the epidermis, in which MTs are substantially restructured and mainly associate with desmosomes (Lechler and Fuchs, 2007; Simpson et al., 2011; Sumigray et al., 2012). Whether Nezha is recruited to desmosomes or remains associated to AJs in the differentiated cells of the epidermis will be an important question to address in the future. This scenario seems similar for CLIP-170 (Stehbens et al., 2006), which is also preferentially expressed in suprabasal epidermal cells (Wacker et al., 1992). Whether MTs can still be targeted to AJs in differentiated mKer and how the association to such different MT-related proteins is regulated in time and space require further investigation and will shed

*, $P < 0.04$; ***, $P < 0.0005$, Student's *t* test. (C) CLASP2-deficient and p120-null mKer with their corresponding controls (scramble and $p120^{f/f}$) were grown with calcium for 4 h followed by addition of 5 μM nocodazole (noc) for 30 min and extraction of monomeric tubulin. Cells were stained for ECad and α-tubulin. (D) Quantification of the number of resistant MTs present at AJs after nocodazole treatment corresponding to C. Only regions with well-formed AJs were selected for the analysis ($n = 30$ cells, 2 independent experiments). Data are normalized to control values and represented as means ± SEM; *, $P < 0.05$; **, $P < 0.002$, Student's *t* test. (E) EB3-GFP was expressed in scramble control cells, CLASP2-deficient cells (CLASP2 knockdown [KD]), p120 control cells ($p120^{f/f}$), and p120-null cells ($p120^{\Delta/\Delta}$). Time-lapse images were taken every 2 s. Individual EB3-GFP comets were manually tracked during the last 12 s before reaching an area of cell–cell contact. The speed in each frame is shown. ($n = 10$ cells; $p120^{f/f}$: 58 MTs; $p120^{\Delta/\Delta}$: 58 MTs; scramble: 59 MTs; CLASP2 knockdown: 74 MTs). Data are represented as means ± SEM; ***, $P < 0.001$; **, $P < 0.01$; *, $P < 0.04$, Student's *t* test. (F) Frequency distribution of MTs showing aberrant trajectories or straight trajectories upon reaching an area of cell–cell contact from the experiment in E. (G) Individual trajectories of EB3-GFP comets in the xy plane were normalized to the last point of the trajectory (corresponding to the time in which EB3-GFP comets reach AJs and fall off the MT). Circles indicate the mean total distance covered by the $p120^{f/f}$ and scramble controls. Bars, 25 μm.

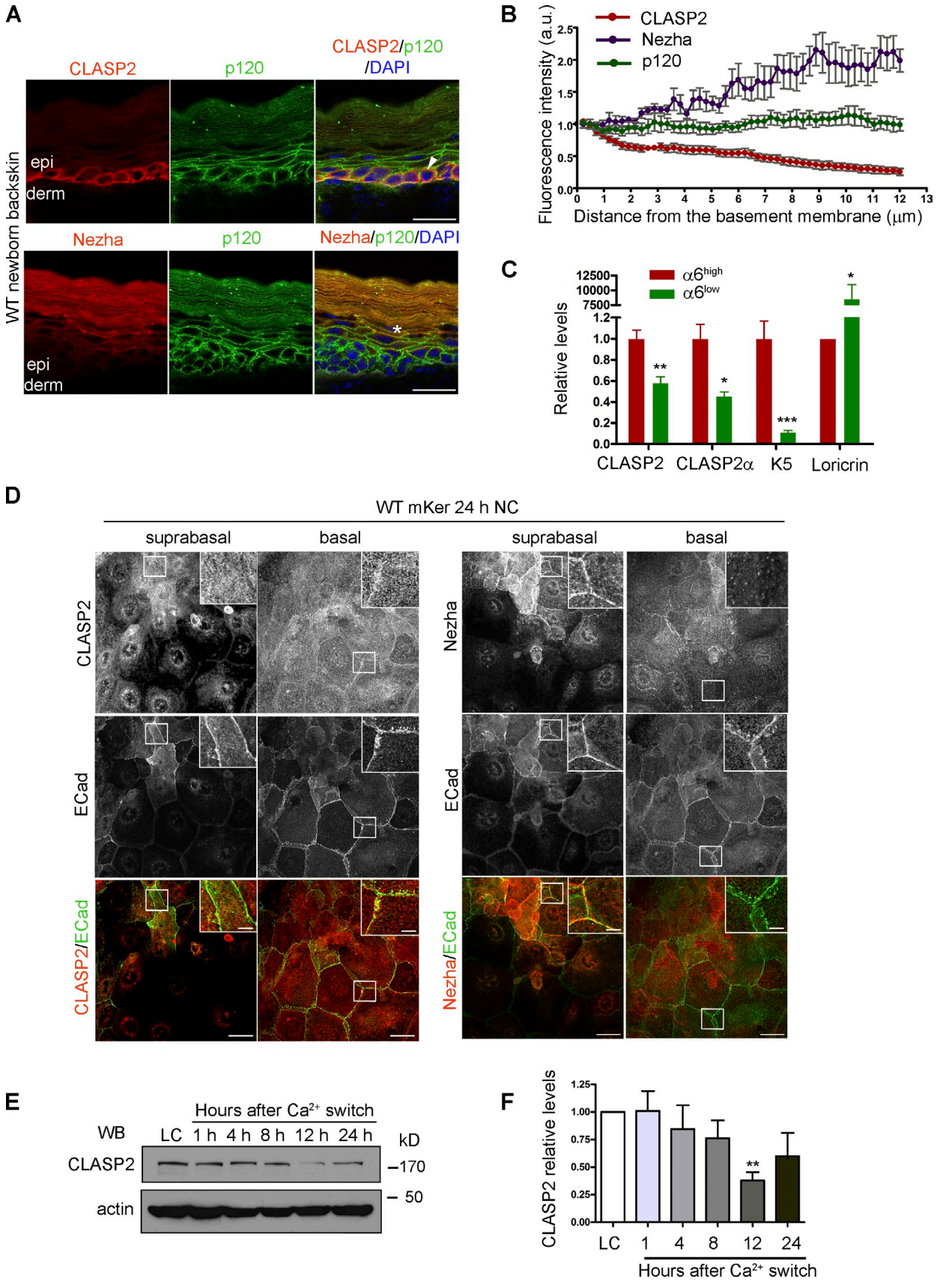

Figure 8. **Differential distribution of CLASP2 and Nezha in the epidermis.** (A) Back skins from WT newborn mice stained for CLASP2/p120 or Nezha/p120. The arrow denotes the basal distribution of CLASP2, and the asterisk indicates suprabasal Nezha localization. epi, epidermis; derm, dermis. (B) Quantification of CLASP2, Nezha, and p120 levels in the epidermis of newborn WT mice. Individual plot profiles were generated across the

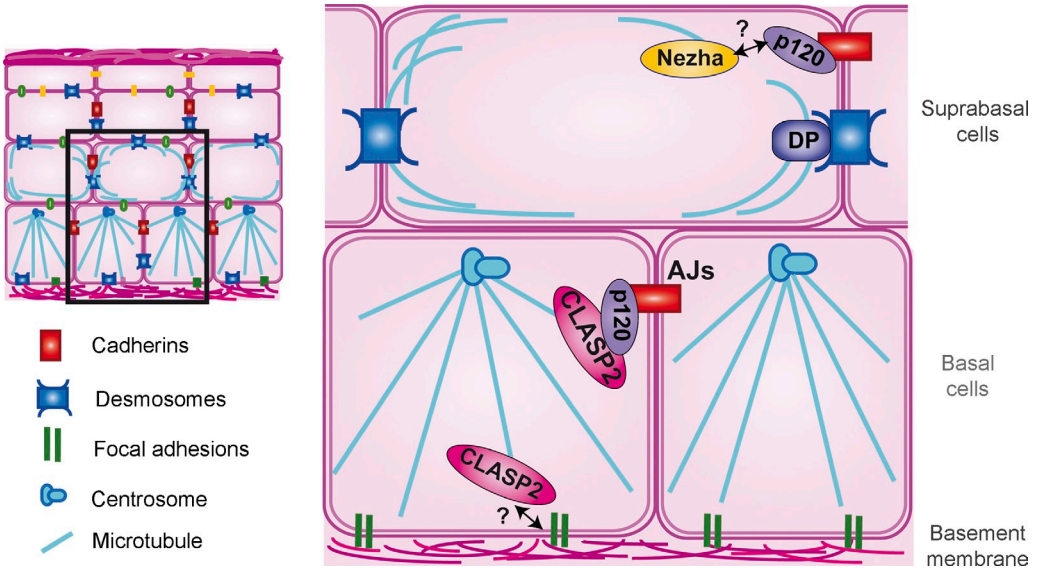

Figure 9. **Proposed model for the p120–CLASP2 interaction at AJs in epidermal basal progenitors.** A scheme of the stratified epidermis is shown, and the magnified area illustrates the microtubule connections with cell adhesions in basal and suprabasal layers. CLASP2 is enriched in basal progenitors, where it targets MTs plus ends to AJs via p120. Nezha localizes in the suprabasal differentiated layers of the epidermis, probably interacting with p120. DP, desmoplakin.

light on the effects of different types of MT-binding proteins on AJ homeostasis.

In closing, our data add a new twist to MT targeting to adhesion sites in the epidermis. In contrast to the previously reported minus-end capture of MTs at desmosomes in differentiating mKer, MT plus ends are targeted to AJs in basal mKer. Moreover, although desmosomes are abundant in nondividing suprabasal cells, AJs play a much more important role in basal cells, in which dynamic junctions must be maintained to facilitate the transition of a proliferative epidermal mKer to a terminally differentiating one, which must exit the basal layer and move upward with its neighbors as a cohesive epithelial sheet. CLASP2 is specifically expressed in these basal cells, in which its association with p120 appears to be key in regulating the MT intercellular connections that govern AJ stability and dynamics in epidermal progenitors.

Materials and methods

Cell culture, transfection, and viral infection

Primary mKer were isolated from newborn mice back skins using dispase (Sigma-Aldrich) and trypsin (Gibco). After filtration in 40-µm cell strainers, cells were cultured in LC medium (0.05 mM Ca^{2+}) containing 15% of Ca^{2+}-depleted FBS as previously described (Nowak and Fuchs, 2009). 293T cells were cultured in DMEM (Gibco) containing 10% FBS. mKer were transfected with Effectene reagent (QIAGEN) according to the manufacturer's instructions, whereas 293T cells were transfected with Lipofectamine 2000 (Invitrogen). 48 h after transfection, the expression of the construct encoding proteins was analyzed by immunoblotting or immunofluorescence.

To ablate p120 expression, $p120^{f/f}$ mKer were infected overnight with 10^7 cfu adenoviruses expressing Cre-GFP or GFP proteins (Cell Biolabs, Inc.) for two consecutive rounds of infection, to achieve in vitro recombination. 4 d after infection, cells were FACS isolated according to their GFP expression levels and cultured or processed for analyses.

CLASP2 expression was down-regulated by infecting mKer overnight with lentiviruses expressing a CLASP2-specific shRNA (clone TRCN0000183632; Sigma-Aldrich) in the presence of 6 µg/ml polybrene (Sigma-Aldrich). 2 d after infection, cells were selected with 400 µg/ml G418 (EMD Millipore). CLASP1 expression was down-regulated by transfecting mKer with a CLASP1 shRNA-pSUPER construct based on the verified sequences for siRNAs against CLASP1 (Mimori-Kiyosue et al., 2005). ECadKO-PCadshRNA mKer, in which ECad KO mKer were transfected with a PCad shRNA construct under the control of the Ker14 (Keratin 14) promoter, have been described elsewhere (Tinkle et al., 2008).

Antibodies

The C terminus of human CLASP2 (nucleotide positions 3,074–3,976 of the KIAA0627 cDNA) was cloned into pGEX4T1 as previously described (Akhmanova et al., 2001), and the resulting fusion protein, GST-hCLASP2, was expressed in BL21 competent bacteria (EMD Millipore) and purified with glutathione–Sepharose beads (GE Healthcare). This fusion protein was used to generate a CLASP2 rabbit polyclonal antibody (Covance), which was affinity purified using the GST-hCLASP2 fusion protein cross-linked to glutathione–Sepharose columns. N. Galjart (Erasmus Medical Center, Rotterdam, Netherlands) provided an additional CLASP2 antibody for validation of specificity. The following antibodies were also used: α-catenin rabbit pAb (C2081; Sigma-Aldrich), α-tubulin mouse mAb (T9026; clone DM1A; Sigma-Aldrich), β-actin mouse mAb (A5441; clone AC-15; Sigma-Aldrich), ECad rat mAb (13–1900; clone ECCD2; Invitrogen), GFP

epidermis, and mean values of fluorescence intensity relative to those expressed at the basement membrane are shown. Data are represented as means ± SEM. (n = 3 mice, 30 plot profiles per mice per staining). a.u., arbitrary unit. (C) Real-time PCR analysis of mKer isolated from the back skin of newborn mice and FACS sorted according to their levels of α6 integrin into two populations: $\alpha6^{high}$ (basal mKer) and $\alpha6^{low}$ (suprabasal mKer). CLASP2 levels were analyzed with two different combinations of primers. Keratin 5 (K5) and loricrin were used as markers of basal and suprabasal mKer, respectively. For each primer pair, values were normalized to the transcript levels of the $\alpha6^{high}$ population. Data are represented as means ± SEM; ***, $P < 0.0004$; **, $P < 0.002$; *, $P < 0.03$, Student's t test. (D) WT mKer subjected to a 24-h calcium switch in vitro and immunostained for either CLASP2 or Nezha together with p120 and ECad. Insets are magnifications of the boxed regions. (E) Immunoblot analysis of CLASP2 levels in WT mKer subjected to a calcium-switch time course for the time points indicated in hours. LC, low calcium. (F) Quantification of CLASP2 levels observed by immunoblotting in D. n = 3 independent experiments. Data are normalized to LC values and represented as means ± SEM; *, $P < 0.008$, Student's t test. Bars: (A and D, main images) 25 µm; (D, insets) 5 µm.

mouse mAb (sc-9996; clone B-2; Santa Cruz Biotechnology, Inc.), GFP rabbit pAb (A11122; Invitrogen), GM130 rat mAb (610822; clone 35/GM130; BD), GST mouse mAb (88D/G4), HA mouse mAb (2367; clone 6E2; Cell Signaling Technology), p120-catenin C-terminal mouse mAb (33–9600; clone 15D2; Invitrogen), p120-catenin N-terminal mouse mAb (33–9700; clone 6H11; Invitrogen), detyrosinated α-tubulin rat mAb (MCA77G; clone YL1/2; AbD Serotec), Nezha rabbit pAb (gift from M. Takeichi, RIKEN Center for Developmental Biology, Chuo-ku, Kobe, Japan; Meng et al., 2008), which recognizes the C-terminal sequence (SRLPG-SRERDWENG) of mouse Nezha, and CLASP1 rabbit pAb (Akhmanova et al., 2001), which recognizes the CLASP1 C terminus (GenBank accession no. AJ288061).

Immunofluorescence and cell treatments

Skins were frozen and embedded in OCT compound. 8-µm sections were fixed in −20°C methanol for 3 min for immunofluorescence stainings. Cells were plated in coverslips and fixed in −20°C methanol for 3 min. Fixed cells were blocked using a blocking buffer containing 0.3% Triton X-100, 1% BSA, 5% normal goat serum, 5% normal donkey serum, and 1% gelatin in PBS. Cells were incubated with primary antibodies according to the manufacturer's instructions followed by incubation with fluorescence-conjugated secondary antibodies (Jackson ImmunoResearch Laboratories, Inc.).

For extraction of monomeric tubulin, cells were washed with an MT-stabilizing buffer (85 mM Pipes, 1 mM EDTA, 1 mM $MgCl_2$, and 2 M glycerol) and extracted with 200 µg/ml saponin dissolved in MT-stabilizing buffer for 5 min before fixation in −20°C methanol as described previously (Gundersen et al., 1987). To fully depolymerize MTs, cells were treated for 4 h with 30 µM nocodazole (Sigma-Aldrich). To determine the population of resistant MTs, cells were treated for 30 min with 5 µM nocodazole followed by extraction of monomeric tubulin. Images were acquired in a confocal microscope (TCS-SP5 Acousto-Optical Beam Splitter; Leica) using an oil immersion objective 63× HCX Plan Apochromat, 1.4 NA with LAS AF v 2.5 software (Leica).

Cell adhesion assays

mKer were switched from LC medium to a medium containing 2 mM Ca^{2+} (NC media) to evaluate AJ formation at different time points. AJ disassembly was evaluated by washing cells with PBS followed by incubation in LC medium.

The adhesion assay to plates coated with Fc-ECad recombinant protein was previously described (Chappuis-Flament et al., 2001). In brief, plates were treated with 100 µg/µl with protein A (GE Healthcare) in PBS during 5 h at 4°C, and nonspecific binding sites were blocked with 0.5% casein hydrolysate enzymatic (ICN Biochemicals) in PBS for 2 h at 4°C. Plates were treated with 0.1 µg/µl Fc-ECad recombinant protein (Sigma-Aldrich) or with 0.1 µg/µl Fc (mouse IgG, Fc fragment; The Jackson Laboratory).

Both scramble controls and CLASP2 knocked down mKer were trypsinized with 0.02% crystalline trypsin (Biological Industries) in PBS with $CaCl_2$ and allowed to attach to the ECad-coated plates for 30 min and 1 h in HBSS with 2 mM $CaCl_2$. Nonadhered cells were washed out, and attached cells were fixed using cold methanol fixation.

The bead adhesion assay was performed as previously described (Perrais et al., 2007), with minor modifications. Protein A polystyrene microspheres (Bangs Laboratories, Inc.) were washed twice with 1 mM sodium acetate, pH 3.9, followed by two washes with 50 mM sodium borate, pH 8.2. Beads were coated with mouse recombinant Fc-ECad at a ratio of 100 µg/100 µl microspheres. Beads were washed with 50 mM sodium acetate, pH 3.9, followed by two washes with 20 mM Hepes, 50 mM NaCl, and 1 mM $CaCl_2$, pH 7.2. Nonspecific binding sites were blocked with 1% BSA for 1 h at 4°C, and beads were resuspended in HBSS with 2 mM $CaCl_2$. WT mKer were incubated with the beads for 5 h in the presence of calcium. Beads coated with the same proportional concentration of IgGs were used as a negative control.

Live-imaging microscopy

To monitor the dynamic movement of CLASP2 to the cortex, WT mKer were transfected with CLASP2-GFP– and p120-cherry–encoding constructs. Cells were switched to NC medium for 5 h. Images were taken at 37°C at 2-s intervals in a laser-scanning confocal microscope (TCS-SP5 Acousto-Optical Beam Splitter) with a water immersion objective 63× HCX Plan Apochromat, 1.2 NA using a temperature-controlled incubator chamber in the presence of CO_2.

To monitor EB3 dynamics at cell–cell contacts, mKer were transfected with a plasmid encoding EB3-GFP and switched to NC medium for 5 h. Images were acquired at 37°C every 2 s in a fluorescent microscope (Eclipse Ti; Nikon) with an oil immersion objective 63× Apochromat total internal reflection fluorescence 60×, NA 1.49, 0.13–0.21 differential interference contrast. Analysis of the EB3 trajectories was performed using Imaris software (Bitplane Scientific Software).

For FRAP experiments, mKer were transfected with the p120-cherry–encoding construct and switched to NC media for 5 h. A constant region of interest (ROI) was defined at the membrane and bleached with a 561-nm laser at 100%. Time-lapse images were acquired at 37°C every 3 s for a total of 64 s. To calculate FRAP curves, a constant region demarcating the membrane was defined within the initial ROI. Bleaching was controlled by examining the fluorescence intensity over time of an unbleached region. Images were taken in a confocal microscope (TCS-SP5 Acousto-Optical Beam Splitter) with a water immersion objective 63× HCX Plan Apochromat, 1.2 NA using a temperature-controlled incubator chamber in the presence of CO_2. Images were analyzed using the confocal microscope software (Leica).

The data were normalized to prebleach values and postbleach values and fitted to the one-phase exponential equation:

$$\text{Fluorescence recovery} = \frac{F(t)-F(0)}{F(-t)-F(0)} = Mf \times \left(1-e^{-\tau t}\right), \text{ and } -\tau = \frac{\ln 0.5}{t_{1/2}},$$

in which $F(t)$ is the mean fluorescence intensity of the selected membrane region within the ROI, $F(0)$ is the postbleach fluorescence intensity, $F(-t)$ is the prebleach fluorescence intensity, Mf is the mobile fraction, and $t_{1/2}$ is the half-life. In every case, 10 µM Hepes was added to the medium to maintain a constant pH.

Protein purification and in vitro pull-down assays

Recombinant p120-GST and Clasp2-GST proteins were expressed in Artic-Express RIL competent bacteria (Agilent Technologies) to avoid degradation of recombinant proteins and purified with glutathione–Sepharose beads. Subsequently, p120-GST fusion proteins were treated overnight with 2 U PreScission Protease (GE Healthcare) per 100 µg of recombinant protein to remove the GST domain. Pull-downs were performed with 1 µg of each recombinant protein in a buffer containing 50 mM Tris, pH 7, 400 mM NaCl, 1 mM EDTA, 1 mM DTT, 10% glycerol, 1% Triton X-100, and PMSF, and samples were analyzed by immunoblotting. Alternatively, p120-GST fusion proteins were used to pull down a lysate of 293T cells transfected with different CLASP2 deletion mutants (Mimori-Kiyosue et al., 2005). Surface membrane proteins were isolated from mKer using a Cell Surface Protein Isolation kit (Thermo Fisher Scientific) following the manufacturer's instructions.

Immunoprecipitations and immunoblot

Immunoprecipitations were performed as previously described (Meng et al., 2008). In brief, mKer lysates were prepared with a buffer containing 50 mM Tris-HCl, pH 7.5, 50 mM NaCl, 0.5 mM EDTA, 0.5 mM EGTA, 1.5 mM $MgCl_2$, 1 mM DTT, and 0.5% Triton X-100. Lysates were incubated overnight with the corresponding antibodies followed by a 1-h incubation with protein G– or A–Sepharose. Proteins were detected by immunoblotting following standard procedures.

Plasmids

For immunofluorescence and live imaging, the following plasmids were used: GFP–CLASP2-α (Akhmanova et al., 2001), EB3-GFP, p120-cherry (generated by cloning the cherry cDNA in frame at the C-terminal end of p120, in a Ker14 promoter vector), and Ker14-ECad-HA (E. Fuchs, The Rockefeller University, New York, NY; Jamora et al., 2003). p120 deletion mutants were generated from the p120-cherry cDNA and cloned into the pHFUW lentiviral expressing vector (gift of O. Fernandez-Capetillo, CNIO, Madrid, Spain) with the HA tag.

For pull-down assays, equivalent deletion mutants were generated by PCR and cloned into pGEX-6P1 (GE Healthcare); in addition, a p120N construct was also generated. CLASP2 deletion mutants were generated by PCR from the GFP–CLASP2-α cDNA and cloned into either the pGEX-4T1 (GE Healthcare) or the pEGFP-C1 plasmid. The list of specific primers used for all the aforementioned constructs is summarized in Table 2.

Flow cytometry, cell sorting, RNA isolation, and real-time PCR

mKer were isolated from the back skin of newborn mice as mentioned in the Cell culture, transfection, and viral infection section. Cell suspensions

Table 2. **List of primers to generate p120 and CLASP2 constructs or to perform quantitative RT-PCR analyses**

Procedure	Primer pair	Forward (5′ → 3′)	Reverse (5′ → 3′)
Cloning into pHFUW-HA tag	p120FL	GAATTCATGGACGACTCAGAGGTGGA	GAATTCTTAAGCGTAGTCTGGGACGTCG TA-TGGGTAAATCTTCTGCATCAAGGG TGC
Cloning into pHFUW-HA tag	p120ΔN	GAATTCATGCCCCCACCTTCAAAC	GAATTCTTAAGCGTAGTCTGGGACGTCG TA-TGGGTAAATCTTCTGCATCAAGGGTGC
Cloning into pGEX-6P1	p120FL	ATAAGAATGCGGCCGCGAATTCATG-GACGACTCAGAGGTGGA	ACGCGTCGACCTGCAGCTAAATCTTCTG-CATCAA
Cloning into pGEX-6P1	p120ΔN	ATAAGAATGCGGCCGCGAATTCATG-CCCCCACCTTCAAAC	ACGCGTCGACCTGCAGCTAAATCTTCTG-CATCAAAA
Cloning into pGEX-6P1	p120N	GAATTCATGGACGACTCAGAGGTGGA	CGGTCGACGAATTCCTACATTCCCTTTCGC-AAACTATCCAA
Cloning into pGEX-4T1	CLASP2FL	TCCCCCGGGAATGGAGCCCCGCAGC-ATGGA	TCCGCGGCCGCCTAACTTTGTCCAGAA-ACATCAGT
Cloning into pGEX-4T1	CLASP2ΔN	TCCCCCGGGAGGAAATCCTGCCAA-CAGTGC	TCCGCGGCCGCCTAACTTTGTCCAGAA-ACATCAGT
Cloning into pGEX-4T1	CLASP2ΔC	TCCCCCGGGAATGGAGCCCCGCA-GCATGGA	TCCGCGGCCGCCTAAGAGCGTGGAG-AGGAGTG
Cloning into pEGFP-C1	CLASP2TOG	GCAGGTACCGCCATGGGAAATCCT-GCCAACAGTGCAAGG	GCACCGCGGTTACCATTTGGAAGAAA-AAGGG
RT-qPCR	Total CLASP2	TTGTCGTCCTCTGTCAGTGC	TGCCACGTCTTCTGTCTGTC
RT-qPCR	CLASP2-α	AAAGAGACATTCCCCCTGCT	TTGCACTGCTGACAGGATTC
RT-qPCR	Keratin 5	CAGTGTGCCAACCTCCAGAACG	AGCCCGCTACCCAAACCAAGAC
RT-qPCR	Loricrin	TCACTCATCTTCCCTGGTGCTT	GTCTTTCCACAACCCACAGGA
RT-qPCR	GAPDH	CGTAGACAAAATGGTGAAGGTCGG	AAGCAGTTGGTGGTGCAGGATG

qPCR, quantitative PCR.

were stained for 30 min at 4°C using a phycoerythrin-conjugated rat anti-CD49f (integrin α6 chain) mAb (555736; clone GoH3; BD) as previously described (Nowak and Fuchs, 2009). Cells were sorted on a FACSAria IIu using the CellQuest Pro software (BD).

Total RNA was isolated from cells using TRIZOL (Invitrogen). After DNase treatment, 2 µg was used for cDNA synthesis using the Ready-To-Go You-Prime First-Strand beads and random primers (GE Healthcare). RT-PCR reactions were conducted using the quantitative PCR master mix (GoTaq; Promega) and a thermal cycler (Mastercycler ep realplex; Eppendorf). The following settings were used: 2 min at 95°C for initial denaturing, 35 cycles of 15 s at 95°C denaturing, 40 s at 57°C annealing, and 45 s at 72°C extension. The expression levels of PCR products were normalized according to GAPDH using specific primers (Table 2).

Quantification and statistical analysis

The levels of ECad and other AJ components at the membrane were analyzed using ImageJ software (National Institutes of Health) as previously described (Verma et al., 2012). In brief, individual lines of constant length were plotted perpendicular to the AJs and used to evaluate peak fluorescence intensity using the PlotProfile feature from ImageJ. The levels of CLASP2 at the membrane, colocalizing with ECad, were analyzed following the same procedure. Random individual plot profiles were generated at AJs using the PlotProfile feature from ImageJ. The CLASP2 peak fluorescence intensity corresponding to the ECad peak fluorescence intensity in the profile was quantified. For MT quantifications, individual MTs were manually counted in cell contact areas and represented as number of MTs per micrometer. The EB3-GFP time-lapse microscopy experiments were analyzed using the Imaris software. Individual EB3-GFP comets were identified using the automatic tools of the Imaris software, and individual tracks were manually quantified. In every set of experiments, all immunofluorescence images were taken under the same exposure conditions. For statistical analysis, the normality of the data was evaluated with a Kolmogorov–Smirnov test. Data that did not present a Gaussian distribution were analyzed using the Mann–Whitney *U* test. Statistical analyses were performed using Prism (GraphPad Software).

Online supplemental material

Fig. S1 shows the specificity of the CLASP2 antibody, along with the analysis of the requirement of cell–cell contact formation for the distribution of CLASP2 to AJs, validated in the absence of cadherins or under LC conditions. Fig. S2 shows the purified recombinant GST-tagged p120 constructs and the CLASP2–p120N protein interaction in yeast. Fig. S3 shows that p120 deficiency does not affect the expression levels and the localization of CLASP2 at MT plus ends but alters its recruitment to AJs at early time points of contact formation. Fig. S4 shows that treatment of mKer with nocodazole does not induce AJ formation per se. Fig. S5 shows that CLASP1 levels are maintained in absence of CLASP2 and that even if CLASP1 only partially localizes to cell–cell contacts, its reductions also lead to a delay in AJ formation. Video 1 shows the dynamic behavior of GFP-CLASP2 after calcium switch at cell–cell adhesion sites. Table S1 summarizes the FRAP analyses results. Online supplemental material is available at http://www.jcb.org/cgi/content/full/jcb.201306019/DC1. Additional data are available in the JCB DataViewer at http://dx.doi.org/10.1083/jcb.201306019.dv.

We thank Terry Lechler (Duke University), Erwin Wagner (CNIO), and the members of the Perez-Moreno laboratory Ljiljana Dukanovic and Donatello Castellana for critical reading of the manuscript. We also thank all members of the BBVA Foundation–CNIO Cancer Cell Biology Program and members of the Gregg Gundersen laboratory for their support and advice. We thank Masatoshi Takeichi for the Nezha antibody and Niels Galjart for providing an additional CLASP2 antibody for validation of specificity. We also thank Francesca Antonucci for technical assistance, Flor Díaz of the mouse facility, the CNIO Flow Cytometry Unit, and the Confocal Microscopy Unit for technical support.

M.N. Shahbazi was a recipient of a CNIO-La Caixa International Ph.D. fellowship. E. Fuchs is an investigator of the Howard Hughes Medical Institute, and additional support for this research came from a grant from the National Institutes of Health (R37-AR27883). The G.G. Gundersen group provided additional support to this research with the National Institutes of Health grant (GM062939). The M. Perez-Moreno group is supported by grants from the Spanish Ministry of Science and Innovation (BFU2009-11885), the Association for International Cancer Research UK (10-0746), and the CNIO (BC1102).

The authors have no conflicting financial interests.

Submitted: 5 June 2013
Accepted: 15 November 2013

References

Akhmanova, A., and M.O. Steinmetz. 2008. Tracking the ends: a dynamic protein network controls the fate of microtubule tips. *Nat. Rev. Mol. Cell Biol.* 9:309–322. http://dx.doi.org/10.1038/nrm2369

Akhmanova, A., C.C. Hoogenraad, K. Drabek, T. Stepanova, B. Dortland, T. Verkerk, W. Vermeulen, B.M. Burgering, C.I. De Zeeuw, F. Grosveld, and

N. Galjart. 2001. Clasps are CLIP-115 and -170 associating proteins involved in the regional regulation of microtubule dynamics in motile fibroblasts. *Cell*. 104:923–935. http://dx.doi.org/10.1016/S0092-8674(01)00288-4

Akhmanova, A., S.J. Stehbens, and A.S. Yap. 2009. Touch, grasp, deliver and control: functional cross-talk between microtubules and cell adhesions. *Traffic*. 10:268–274. http://dx.doi.org/10.1111/j.1600-0854.2008.00869.x

Bacallao, R., C. Antony, C. Dotti, E. Karsenti, E.H. Stelzer, and K. Simons. 1989. The subcellular organization of Madin-Darby canine kidney cells during the formation of a polarized epithelium. *J. Cell Biol.* 109:2817–2832. http://dx.doi.org/10.1083/jcb.109.6.2817

Bartolini, F., and G.G. Gundersen. 2006. Generation of noncentrosomal microtubule arrays. *J. Cell Sci.* 119:4155–4163. http://dx.doi.org/10.1242/jcs.03227

Bellett, G., J.M. Carter, J. Keynton, D. Goldspink, C. James, D.K. Moss, and M.M. Mogensen. 2009. Microtubule plus-end and minus-end capture at adherens junctions is involved in the assembly of apico-basal arrays in polarised epithelial cells. *Cell Motil. Cytoskeleton*. 66:893–908. http://dx.doi.org/10.1002/cm.20393

Chappuis-Flament, S., E. Wong, L.D. Hicks, C.M. Kay, and B.M. Gumbiner. 2001. Multiple cadherin extracellular repeats mediate homophilic binding and adhesion. *J. Cell Biol.* 154:231–243. http://dx.doi.org/10.1083/jcb.200103143

Chausovsky, A., A.D. Bershadsky, and G.G. Borisy. 2000. Cadherin-mediated regulation of microtubule dynamics. *Nat. Cell Biol.* 2:797–804. http://dx.doi.org/10.1038/35041037

Chen, X., S. Kojima, G.G. Borisy, and K.J. Green. 2003. p120 catenin associates with kinesin and facilitates the transport of cadherin–catenin complexes to intercellular junctions. *J. Cell Biol.* 163:547–557. http://dx.doi.org/10.1083/jcb.200305137

Curtis, M.W., K.R. Johnson, and M.J. Wheelock. 2008. E-cadherin/catenin complexes are formed cotranslationally in the endoplasmic reticulum/Golgi compartments. *Cell Commun. Adhes.* 15:365–378. http://dx.doi.org/10.1080/15419060802460748

Davis, M.A., R.C. Ireton, and A.B. Reynolds. 2003. A core function for p120-catenin in cadherin turnover. *J. Cell Biol.* 163:525–534. http://dx.doi.org/10.1083/jcb.200307111

Desai, A., and T.J. Mitchison. 1997. Microtubule polymerization dynamics. *Annu. Rev. Cell Dev. Biol.* 13:83–117. http://dx.doi.org/10.1146/annurev.cellbio.13.1.83

Drabek, K., M. van Ham, T. Stepanova, K. Draegestein, R. van Horssen, C.L. Sayas, A. Akhmanova, T. Ten Hagen, R. Smits, R. Fodde, et al. 2006. Role of CLASP2 in microtubule stabilization and the regulation of persistent motility. *Curr. Biol.* 16:2259–2264. http://dx.doi.org/10.1016/j.cub.2006.09.065

Efimov, A., A. Kharitonov, N. Efimova, J. Loncarek, P.M. Miller, N. Andreyeva, P. Gleeson, N. Galjart, A.R. Maia, I.X. McLeod, et al. 2007. Asymmetric CLASP-dependent nucleation of noncentrosomal microtubules at the trans-Golgi network. *Dev. Cell*. 12:917–930. http://dx.doi.org/10.1016/j.devcel.2007.04.002

Franz, C.M., and A.J. Ridley. 2004. p120 catenin associates with microtubules: inverse relationship between microtubule binding and Rho GTPase regulation. *J. Biol. Chem.* 279:6588–6594. http://dx.doi.org/10.1074/jbc.M312812200

Gundersen, G.G. 2002. Evolutionary conservation of microtubule-capture mechanisms. *Nat. Rev. Mol. Cell Biol.* 3:296–304. http://dx.doi.org/10.1038/nrm777

Gundersen, G.G., S. Khawaja, and J.C. Bulinski. 1987. Postpolymerization detyrosination of α-tubulin: a mechanism for subcellular differentiation of microtubules. *J. Cell Biol.* 105:251–264. http://dx.doi.org/10.1083/jcb.105.1.251

Hotta, A., T. Kawakatsu, T. Nakatani, T. Sato, C. Matsui, T. Sukezane, T. Akagi, T. Hamaji, I. Grigoriev, A. Akhmanova, et al. 2010. Laminin-based cell adhesion anchors microtubule plus ends to the epithelial cell basal cortex through LL5α/β. *J. Cell Biol.* 189:901–917. http://dx.doi.org/10.1083/jcb.200910095

Howard, J., and A.A. Hyman. 2009. Growth, fluctuation and switching at microtubule plus ends. *Nat. Rev. Mol. Cell Biol.* 10:569–574. http://dx.doi.org/10.1038/nrm2713

Ichii, T., and M. Takeichi. 2007. p120-catenin regulates microtubule dynamics and cell migration in a cadherin-independent manner. *Genes Cells*. 12:827–839. http://dx.doi.org/10.1111/j.1365-2443.2007.01095.x

Ishiyama, N., S.H. Lee, S. Liu, G.Y. Li, M.J. Smith, L.F. Reichardt, and M. Ikura. 2010. Dynamic and static interactions between p120 catenin and E-cadherin regulate the stability of cell-cell adhesion. *Cell*. 141:117–128. http://dx.doi.org/10.1016/j.cell.2010.01.017

Ivanov, A.I., I.C. McCall, B. Babbin, S.N. Samarin, A. Nusrat, and C.A. Parkos. 2006. Microtubules regulate disassembly of epithelial apical junctions. *BMC Cell Biol.* 7:12. http://dx.doi.org/10.1186/1471-2121-7-12

Jamora, C., R. DasGupta, P. Kocieniewski, and E. Fuchs. 2003. Links between signal transduction, transcription and adhesion in epithelial bud development. *Nature*. 422:317–322. http://dx.doi.org/10.1038/nature01458

Karakesisoglou, I., Y. Yang, and E. Fuchs. 2000. An epidermal plakin that integrates actin and microtubule networks at cellular junctions. *J. Cell Biol.* 149:195–208. http://dx.doi.org/10.1083/jcb.149.1.195

Kee, S.H., and P.M. Steinert. 2001. Microtubule disruption in keratinocytes induces cell-cell adhesion through activation of endogenous E-cadherin. *Mol. Biol. Cell*. 12:1983–1993. http://dx.doi.org/10.1091/mbc.12.7.1983

Lansbergen, G., I. Grigoriev, Y. Mimori-Kiyosue, T. Ohtsuka, S. Higa, I. Kitajima, J. Demmers, N. Galjart, A.B. Houtsmuller, F. Grosveld, and A. Akhmanova. 2006. CLASPs attach microtubule plus ends to the cell cortex through a complex with LL5beta. *Dev. Cell*. 11:21–32. http://dx.doi.org/10.1016/j.devcel.2006.05.012

Lechler, T., and E. Fuchs. 2007. Desmoplakin: an unexpected regulator of microtubule organization in the epidermis. *J. Cell Biol.* 176:147–154. http://dx.doi.org/10.1083/jcb.200609109

Ligon, L.A., S. Karki, M. Tokito, and E.L. Holzbaur. 2001. Dynein binds to beta-catenin and may tether microtubules at adherens junctions. *Nat. Cell Biol.* 3:913–917. http://dx.doi.org/10.1038/ncb1001-913

Long, J.B., M. Bagonis, L.A. Lowery, H. Lee, G. Danuser, and D. Van Vactor. 2013. Multiparametric analysis of CLASP-interacting protein functions during interphase microtubule dynamics. *Mol. Cell. Biol.* 33:1528–1545. http://dx.doi.org/10.1128/MCB.01442-12

Lüders, J., and T. Stearns. 2007. Microtubule-organizing centres: a re-evaluation. *Nat. Rev. Mol. Cell Biol.* 8:161–167. http://dx.doi.org/10.1038/nrm2100

Mariner, D.J., J. Wang, and A.B. Reynolds. 2000. ARVCF localizes to the nucleus and adherens junction and is mutually exclusive with p120(ctn) in E-cadherin complexes. *J. Cell Sci.* 113:1481–1490.

Mary, S., S. Charrasse, M. Meriane, F. Comunale, P. Travo, A. Blangy, and C. Gauthier-Rouvière. 2002. Biogenesis of N-cadherin-dependent cell-cell contacts in living fibroblasts is a microtubule-dependent kinesin-driven mechanism. *Mol. Biol. Cell*. 13:285–301. http://dx.doi.org/10.1091/mbc.01-07-0337

Meng, W., Y. Mushika, T. Ichii, and M. Takeichi. 2008. Anchorage of microtubule minus ends to adherens junctions regulates epithelial cell-cell contacts. *Cell*. 135:948–959. http://dx.doi.org/10.1016/j.cell.2008.09.040

Miller, P.M., A.W. Folkmann, A.R. Maia, N. Efimova, A. Efimov, and I. Kaverina. 2009. Golgi-derived CLASP-dependent microtubules control Golgi organization and polarized trafficking in motile cells. *Nat. Cell Biol.* 11:1069–1080 http://dx.doi.org/10.1038/ncb1920

Mimori-Kiyosue, Y., I. Grigoriev, G. Lansbergen, H. Sasaki, C. Matsui, F. Severin, N. Galjart, F. Grosveld, I. Vorobjev, S. Tsukita, and A. Akhmanova. 2005. CLASP1 and CLASP2 bind to EB1 and regulate microtubule plus-end dynamics at the cell cortex. *J. Cell Biol.* 168:141–153. http://dx.doi.org/10.1083/jcb.200405094

Nowak, J.A., and E. Fuchs. 2009. Isolation and culture of epithelial stem cells. *Methods Mol. Biol.* 482:215–232.

Olmsted, J.B., and G.G. Borisy. 1973. Microtubules. *Annu. Rev. Biochem.* 42:507–540. http://dx.doi.org/10.1146/annurev.bi.42.070173.002451

Paulson, A.F., E. Mooney, X. Fang, H. Ji, and P.D. McCrea. 2000. Xarvcf, *Xenopus* member of the p120 catenin subfamily associating with cadherin juxtamembrane region. *J. Biol. Chem.* 275:30124–30131. http://dx.doi.org/10.1074/jbc.M003048200

Perez-Moreno, M., M.A. Davis, E. Wong, H.A. Pasolli, A.B. Reynolds, and E. Fuchs. 2006. p120-catenin mediates inflammatory responses in the skin. *Cell*. 124:631–644. http://dx.doi.org/10.1016/j.cell.2005.11.043

Perrais, M., X. Chen, M. Perez-Moreno, and B.M. Gumbiner. 2007. E-cadherin homophilic ligation inhibits cell growth and epidermal growth factor receptor signaling independently of other cell interactions. *Mol. Biol. Cell*. 18:2013–2025. http://dx.doi.org/10.1091/mbc.E06-04-0348

Ruiz-Saenz, A., J. van Haren, C. Laura Sayas, L. Rangel, J. Demmers, J. Millán, M.A. Alonso, N. Galjart, and I. Correas. 2013. Protein 4.1R binds to CLASP2 and regulates dynamics, organization and attachment of microtubules to the cell cortex. *J. Cell Sci.* 126:4589–4601. http://dx.doi.org/10.1242/jcs.120840

Simpson, C.L., D.M. Patel, and K.J. Green. 2011. Deconstructing the skin: cytoarchitectural determinants of epidermal morphogenesis. *Nat. Rev. Mol. Cell Biol.* 12:565–580. http://dx.doi.org/10.1038/nrm3175

Stehbens, S.J., A.D. Paterson, M.S. Crampton, A.M. Shewan, C. Ferguson, A. Akhmanova, R.G. Parton, and A.S. Yap. 2006. Dynamic microtubules regulate the local concentration of E-cadherin at cell-cell contacts. *J. Cell Sci.* 119:1801–1811. http://dx.doi.org/10.1242/jcs.02903

Stepanova, T., J. Slemmer, C.C. Hoogenraad, G. Lansbergen, B. Dortland, C.I. De Zeeuw, F. Grosveld, G. van Cappellen, A. Akhmanova, and N. Galjart. 2003. Visualization of microtubule growth in cultured neurons

via the use of EB3-GFP (end-binding protein 3-green fluorescent protein). *J. Neurosci.* 23:2655–2664.

Sumigray, K.D., H. Chen, and T. Lechler. 2011. Lis1 is essential for cortical microtubule organization and desmosome stability in the epidermis. *J. Cell Biol.* 194:631–642. http://dx.doi.org/10.1083/jcb.201104009

Sumigray, K.D., H.P. Foote, and T. Lechler. 2012. Noncentrosomal microtubules and type II myosins potentiate epidermal cell adhesion and barrier formation. *J. Cell Biol.* 199:513–525. http://dx.doi.org/10.1083/jcb.201206143

Tinkle, C.L., H.A. Pasolli, N. Stokes, and E. Fuchs. 2008. New insights into cadherin function in epidermal sheet formation and maintenance of tissue integrity. *Proc. Natl. Acad. Sci. USA*. 105:15405–15410. http://dx.doi.org/10.1073/pnas.0807374105

Tsvetkov, A.S., A. Samsonov, A. Akhmanova, N. Galjart, and S.V. Popov. 2007. Microtubule-binding proteins CLASP1 and CLASP2 interact with actin filaments. *Cell Motil. Cytoskeleton*. 64:519–530. http://dx.doi.org/10.1002/cm.20201

Vasioukhin, V., C. Bauer, M. Yin, and E. Fuchs. 2000. Directed actin polymerization is the driving force for epithelial cell-cell adhesion. *Cell*. 100:209–219. http://dx.doi.org/10.1016/S0092-8674(00)81559-7

Verma, S., S.P. Han, M. Michael, G.A. Gomez, Z. Yang, R.D. Teasdale, A. Ratheesh, E.M. Kovacs, R.G. Ali, and A.S. Yap. 2012. A WAVE2-Arp2/3 actin nucleator apparatus supports junctional tension at the epithelial zonula adherens. *Mol. Biol. Cell*. 23:4601–4610. http://dx.doi.org/10.1091/mbc.E12-08-0574

Wacker, I.U., J.E. Rickard, J.R. De Mey, and T.E. Kreis. 1992. Accumulation of a microtubule-binding protein, pp170, at desmosomal plaques. *J. Cell Biol.* 117:813–824. http://dx.doi.org/10.1083/jcb.117.4.813

Watanabe, T., J. Noritake, M. Kakeno, T. Matsui, T. Harada, S. Wang, N. Itoh, K. Sato, K. Matsuzawa, A. Iwamatsu, et al. 2009. Phosphorylation of CLASP2 by GSK-3beta regulates its interaction with IQGAP1, EB1 and microtubules. *J. Cell Sci.* 122:2969–2979. http://dx.doi.org/10.1242/jcs.046649

Waterman-Storer, C.M., W.C. Salmon, and E.D. Salmon. 2000. Feedback interactions between cell-cell adherens junctions and cytoskeletal dynamics in newt lung epithelial cells. *Mol. Biol. Cell*. 11:2471–2483. http://dx.doi.org/10.1091/mbc.11.7.2471

Xiao, K., R.G. Oas, C.M. Chiasson, and A.P. Kowalczyk. 2007. Role of p120-catenin in cadherin trafficking. *Biochim. Biophys. Acta*. 1773:8–16. http://dx.doi.org/10.1016/j.bbamcr.2006.07.005

Yanagisawa, M., I.N. Kaverina, A. Wang, Y. Fujita, A.B. Reynolds, and P.Z. Anastasiadis. 2004. A novel interaction between kinesin and p120 modulates p120 localization and function. *J. Biol. Chem.* 279:9512–9521. http://dx.doi.org/10.1074/jbc.M310895200

Yap, A.S., B.R. Stevenson, K.C. Abel, E.J. Cragoe Jr., and S.W. Manley. 1995. Microtubule integrity is necessary for the epithelial barrier function of cultured thyroid cell monolayers. *Exp. Cell Res.* 218:540–550. http://dx.doi.org/10.1006/excr.1995.1189